

# Assessment of wave run-up reduction by salt marshes



Timor M.I. Post

*8<sup>th</sup> of October 2015*

**UNIVERSITY OF TWENTE.**





## **Assessment of wave run-up reduction by salt marshes**

Submitted to acquire the degree of Master of Science at the University of Twente.

Author Timor M.I. Post  
Date October 8<sup>th</sup> 2015  
Email t.m.i.post@student.utwente.com

### Supervisors

*HKV*

Daily supervisor: Ir. V. Vuik

*University of Twente*

University supervisor: Dr. ir. B.W. Borsje

University professor: Prof. dr. S.J.H.M. Hulscher

### Project

BE SAFE



## Abstract

The purpose of this thesis is to analyze the salt marshes in the eastern Wadden Sea which are located in front of the dike and assess how these areas influence the waves. Additionally, this thesis looks into the uses of flotsam lines. These lines are made up of pieces of floating debris (or: flotsam) which are transported by waves and left on the slope of a dike, marking the maximum wave run-up for a dike section. The reason for this research is that in evaluations of the required height and strength of a dike, the salt marshes are not taken into account. This means that the design of these dikes is oversized and costly. By determining the impact of the salt marshes on wave conditions under design conditions, it is possible to reduce the uncertainties and take the effects of the salt marshes into account in future dike safety evaluations. Dikes could be deemed 'safe' for additional decades, saving up to several million euro per kilometer of shoreline. The flotsam lines are a low-cost source of information and by showing the possible use of this method, valuable data can be gathered after a storm passes in locations where no wave measurements are available.

Chapter 1 is the introductory chapter, which starts with a motivation for the research into these topics. The second part gives the context under which this research is performed, since the thesis is based on measurements which were collected in the Eastern Wadden Sea during and after the storm of January 11<sup>th</sup> 2015. This leads to the problem statement, objectives, research questions and methodology.

Chapter 2 describes the methods which will be used during the research. The two models are shortly introduced. The other topic which requires a clear introduction is the calculation of the maximum wave run-up. This approach is necessary to relate the waves from the 2D model to the measured flotsam lines.

Chapter 3 presents the location and the different measurements which were collected for this research. The different measurements consist of pressure gauges, which recorded the water level and wave characteristics at the salt marsh, and the flotsam lines. The first findings are done in this chapter. This is based on the flotsam lines and conditions of the foreshore, and the differences in measured wave heights for the different pressure gauges.

Chapter 4 describes the settings and results of the 1D and 2D model in detail. These models are first used to replicate the wave measurements and are then scaled up to design conditions.

The flotsam levels are replicated in Chapter 5. This is done using the results from the calibrated 2D model and the approach for the maximum wave run-up explained in Chapter 2.

In Chapter 6 the two models are subjected to a scenario analysis where design conditions for the local dike section are applied and characteristics such as vegetation and the bed level are changed. This is needed to answer the research question related to the influence of the salt marshes during design conditions.

In Chapter 7 the results and several topics encountered during the research are discussed.

Conclusions are drawn in Chapter 8, ending with several recommendations for future research. The research questions raised regarding the influence of the salt marsh on local wave conditions and the possibilities with the flotsam lines are answered. What was found in this research is that the salt marshes have a significant impact on the wave height during design conditions, reducing wave run-up by up to 41%. The analysis in Chapter 3 of the flotsam lines, compared to the foreshore characteristics showed that the flotsam lines are a good indicator for local wave conditions. Additionally, the shape of the flotsam lines is replicated with results from the 2D model. However, it was not possible to replicate the exact values of the flotsam lines for all measured points. This is caused by a combination of uncertainties related to both the model and the measurements.

## Samenvatting

Het doel van deze thesis is het analyseren van de kwelders die voor de dijk liggen in de oostelijke Waddenzee en daarbij bepalen hoe deze gebieden de golven beïnvloeden. Bovendien onderzoekt deze thesis mogelijke gebieden van de veekranden. Deze lijnen bestaan uit drijvende deeltjes welke achtergelaten worden op het talud van de dijk tijdens een storm door de golven. Deze lijn markeert de maximale lokale golfoploop. De reden voor dit onderzoek is dat bij de evaluaties van de benodigde hoogte en sterkte van een dijk, kwelders niet in de berekeningen worden meegenomen. Dit leidt tot overgedimensioneerde dijken wat hoge kosten tot gevolg heeft. Door het bepalen van de invloed van deze kwelders op de golfcondities onder ontwerpcondities, wordt het mogelijk om onzekerheden op dit gebied te verkleinen en de invloed van de kwelders mee te nemen in veiligheidsevaluaties. Dit kan ervoor zorgen dat de levensduur van huidige dijken met enkele decennia verlengd kan worden, op klein onderhoud na, wat een besparing kan opleveren van enkele miljoenen euro per km. De veekranden zijn een kosten-efficiënte bron van informatie en door het aantonen van de mogelijkheden kan waardevolle data over een storm in de toekomst toch verzameld worden, zelfs wanneer er geen andere metingen zijn in een gebied.

Hoofdstuk 1 is het inleidende hoofdstuk, welke begint met de aanleiding voor het onderzoek naar deze onderwerpen. Het tweede gedeelte geeft de context van dit onderzoek weer, aangezien deze thesis bouwt op metingen die in de oostelijke Waddenzee waren verzameld tijdens en na de storm van 11 januari 2015. Dit leidt tot de probleemstelling, doelen, onderzoeksvragen en methodologie.

Hoofdstuk 2 beschrijft de methoden welke in dit onderzoek gebruikt worden. De twee modellen worden kort geïntroduceerd. Het andere onderwerp wat een duidelijke uitleg nodig heeft is de berekening voor de maximale golfoploop. Deze berekeningsmethode is nodig om de berekende golven uit het 2D model te koppelen aan de veekranden.

Hoofdstuk 3 beschrijft de locatie en de verschillende metingen welke gedaan zijn voor dit onderzoek. De metingen bestaan uit de veekranden en druksensoren. Deze sensoren zijn gebruikt om de waterdiepte en golfeigenschappen te bepalen. De eerste bevindingen worden in dit hoofdstuk gedaan. Dit is gebaseerd op de veekranden en de condities van het voorland, en het verschil in gemeten golfhoogtes tussen de verschillende sensoren.

Hoofdstuk 4 beschrijft de instellingen en resultaten van het 1D en 2D model in detail. Deze modellen worden eerst gebruikt om de golfmetingen te reproduceren en worden vervolgens opgeschaald naar de ontwerpcondities.

De veekranden worden gereproduceerd in hoofdstuk 5. Dit wordt gedaan met behulp van de resultaten uit het 2D model en de aanpak voor de maximale golfloop, beschreven in hoofdstuk 2.

In hoofdstuk 6 worden de twee modellen onderworpen aan een scenario analyse waarbij lokale ontwerpcondities voor de dijk worden toegepast en eigenschappen zoals vegetatie en bodem niveau worden aangepast. Dit is noodzakelijk om de onderzoeksvraag met betrekking tot de invloed van de kwelders tijdens ontwerpcondities te beantwoorden.

Tijdens de discussie in hoofdstuk 7 worden de resultaten besproken alsook een aantal onderwerpen die tijdens het onderzoek werden opgemerkt.

Conclusies worden besproken in hoofdstuk 8, eindigend met een aanbevelingen voor toekomstig onderzoek. De opgestelde onderzoeksvragen met betrekking tot de invloed van de kwelders op golfdemping en de mogelijkheden voor het gebruik van de veekranden worden hier beantwoord. Wat in dit onderzoek werd bevonden is dat de kwelders een significante invloed hebben op de golfhoogte bij ontwerpcondities, waarbij de golfloop met maximaal 41% werd gereduceerd. De analyse van de veekranden in hoofdstuk 3 laat zien dat de veekranden een goede indicator is voor lokale golfcondities. Bij het reproduceren van de veekranden bleek dat de vorm van de metingen goed volgde uit de berekeningen, maar dat het niet mogelijk was om de exacte waarden van de veekranden voor alle locaties te reproduceren. Dit wordt veroorzaakt door een combinatie van meerdere bronnen van onzekerheden.

## Preface

Over the last several months I have worked on this master thesis research called “*Assessment of wave run-up reduction by salt marshes*”. Completing this research will finalize my master study Water Engineering and Management at the University of Twente. The company HKV where I worked during this time is a positive environment with friendly, capable and helpful people. Among the students there was good atmosphere which always allowed for a chat about our common issues and with this group we even ran a marathon in the charity run *Lijn in Waterloop* organized by the company, which was a lot of fun.

I would like to thank Bas Borsje for his confidence in me to start this assignment in the first place and helping me along the way. I would also like to thank my professor Suzanne Hulscher for her time, energy and feedback. Special thanks must go to my daily supervisor Vincent Vuik for his ability to always spot the source of problems and helping me on many moments during my research. Although I encountered plenty of difficulties along the way, both supervisors kept me on track and helped me out where necessary.

Timor Post, October 8<sup>th</sup> 2015

# Table of contents

Abstract.....	i
Samenvatting .....	iii
Preface.....	v
1. Introduction .....	1
1.1. Context.....	3
1.2. Problem statement .....	5
1.3. Objectives and research questions.....	6
1.4. Methodology.....	7
2. Methods .....	9
2.1. Modelling Setup .....	9
2.2. Wave run-up calculation .....	13
3. Measurements .....	16
3.1 Location .....	16
3.2 Pressure gauges .....	18
3.3 Flotsam lines .....	21
3.4 Summary.....	24
4. Models .....	25
4.1. 1D model.....	25
4.2. 2D model.....	35
5. Flotsam level reproduction .....	47
Summary .....	51
6. Scenario analysis .....	52
6.1. Scenarios .....	52
6.2. 1D scenario results.....	54
6.3. 2D scenario results.....	56
7. Discussion.....	61

8. Conclusions and recommendations.....	63
References.....	65
Appendix A: Source terms of the 1D scenarios.....	67
Appendix B: Source terms of the 2D scenarios.....	70



## 1. Introduction

Countries around the world protect their shores from the influences of the seas and oceans. The dikes which are often needed to prevent the coastal areas from flooding require evaluation in order to ensure that the desired level of protection is achieved. Different failure mechanisms should be taken into account such as erosion of the outer or inner slope, piping, micro-instability and wave overtopping (Figure 1). By lowering the chance of failure by these mechanisms, the level of safety of a dike is increased. When a dike section is determined to be unsafe, this means that the probability that one or more of the failure mechanisms occur is too high. To increase the safety of a dike section, engineers can increase the strength and height of a dike or lower the load caused by the water level and wave conditions.

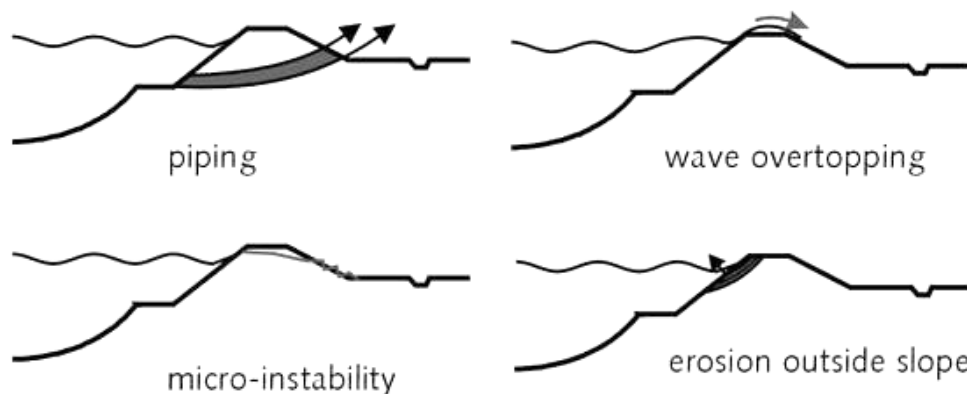
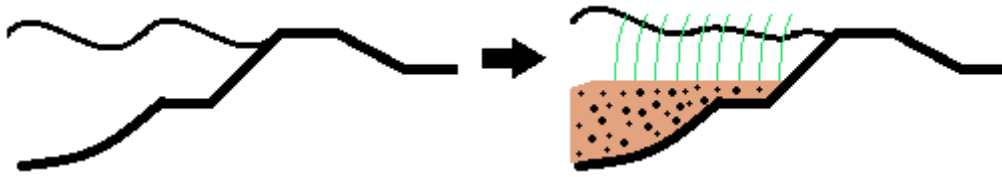


Figure 1 Several failure mechanisms for a dike (Figure source: Deltares)

Increasing the bed level in front of a dike in combination with planting vegetation (or: a vegetated foreshore) is one of the options to lower the wave heights at a dike (Venema, Schelfhout, Moerman, & van Duren, 2012). The possible types of vegetation can be very different, ranging from reed to grass or even trees such as willows. An example found in tropical climates are mangrove forests which are naturally occurring forests and have a positive effect on the amount of wave-damping and sedimentation (Horstman et al., 2014). The presence of a vegetated foreshore (Figure 2) in front of a dike section reduces the probability for several failure mechanisms such as overtopping, piping, erosion of the inner and outer and micro- and macro-instability (Venema et al., 2012). An additional positive effect of a vegetated foreshore are the benefits for natural and landscape values.



**Figure 2 A vegetated foreshore dampens the incoming waves**

The type of vegetated foreshore which is the focus of this research are the salt marshes in the eastern Wadden Sea (in Dutch: kwelders). The salt marshes in this area have different types of vegetation which is highly dependent on the bed level. The area at the edge of the salt marsh is inundated at each high tide due to the low bed level and is known as the pioneer zone. The pioneer zone is mostly inhabited by *Salicornia* *Spartina*. The areas which are inundated less frequently than 400 times and less than 100 times per year are dominated by respectively *Puccinellia Halimione* and *Festuca Juncus* (Dijkema, Duin, Dijkman, & Leeuwen, 2007).

An event which can occur during a storm, is the generation of flotsam lines (in Dutch: veekranden) on the dikes (Figure 3). The wind and waves generated by the storm event transport floating material (or flotsam) towards the dike. The waves which run up the dike then leave this flotsam on the slope of the dike, marking the highest wave run-up. In the past, flotsam level measurements have been used as a direct indicator of how the wave conditions varied along the dike (Grüne, 2005).



**Figure 3 On the left is the Wadden Sea and one of the salt marshes. On the dike there is a clearly visible flotsam line all along the length of the dike (Photo by: Vincent Vuik)**

## 1.1. Context

The project BE SAFE investigates wave damping by vegetation to find the real influence of vegetation on wave-damping. By doing this, the goal is to quantify uncertainties related to vegetated foreshores and make it a reliable “building with nature” option to achieve wave height reduction. This thesis is performed as part of this project.

In the eastern Dutch Wadden Sea, salt marshes cover large parts of the mainland coast reaching up to 650 meters seawards. For the most eastward location of the salt marshes, several pressure sensors were placed both inside the vegetation and on barren areas to determine the effect of the salt marshes on waves. These sensors measured the water level and waves during the storm which peaked on January 11<sup>th</sup> 2015. In order to quantify the wave-damping on salt marshes, it is necessary to know how the waves behaved on the salt-marsh. This makes these measurements crucial to the research.

The flotsam height was measured after the storm of January 11<sup>th</sup> passed. This research will make use of the flotsam levels as an indicator of wave intensity and show how the flotsam levels can be related to the wave conditions.

Preceding January 11<sup>th</sup> 2015, a low pressure field passed over the North Sea which resulted in wind bursts up to 30 m/s, and wind speed hourly averages of approximately 16 km/h directed from west to east (Figure 4). The storm surge increased the water level to 2.97 m +NAP in the eastern Wadden Sea. For comparison, the regular daily maximum is between 1 and 1.50 meters +NAP. The significant wave height  $H_{m0}$  measured at the buoy north of the barrier island Schiermonnikoog increased to 7 meters (Figure 5), while during calm days this varies between 1 and 1.5 meters. Due to the measurements taken during and after this storm, valuable data is available. Without these measurements, the investigation of wave-damping on the salt marshes would not be possible.

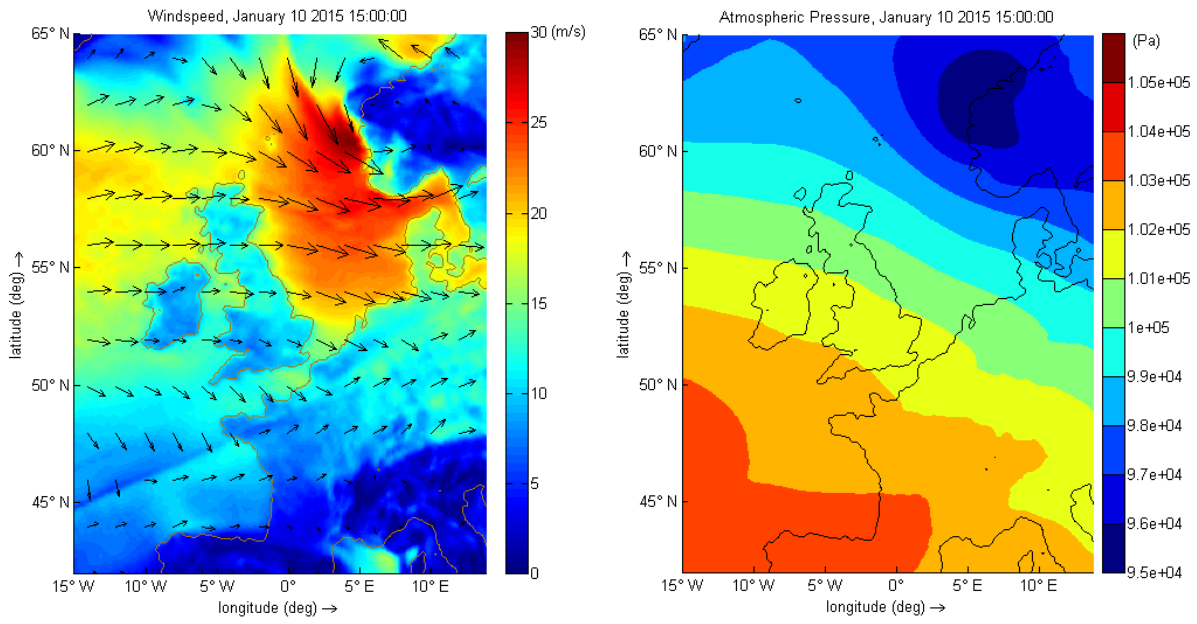


**Figure 4** Wind speed and atmospheric pressure field calculated by the meteorological model HIRLAM

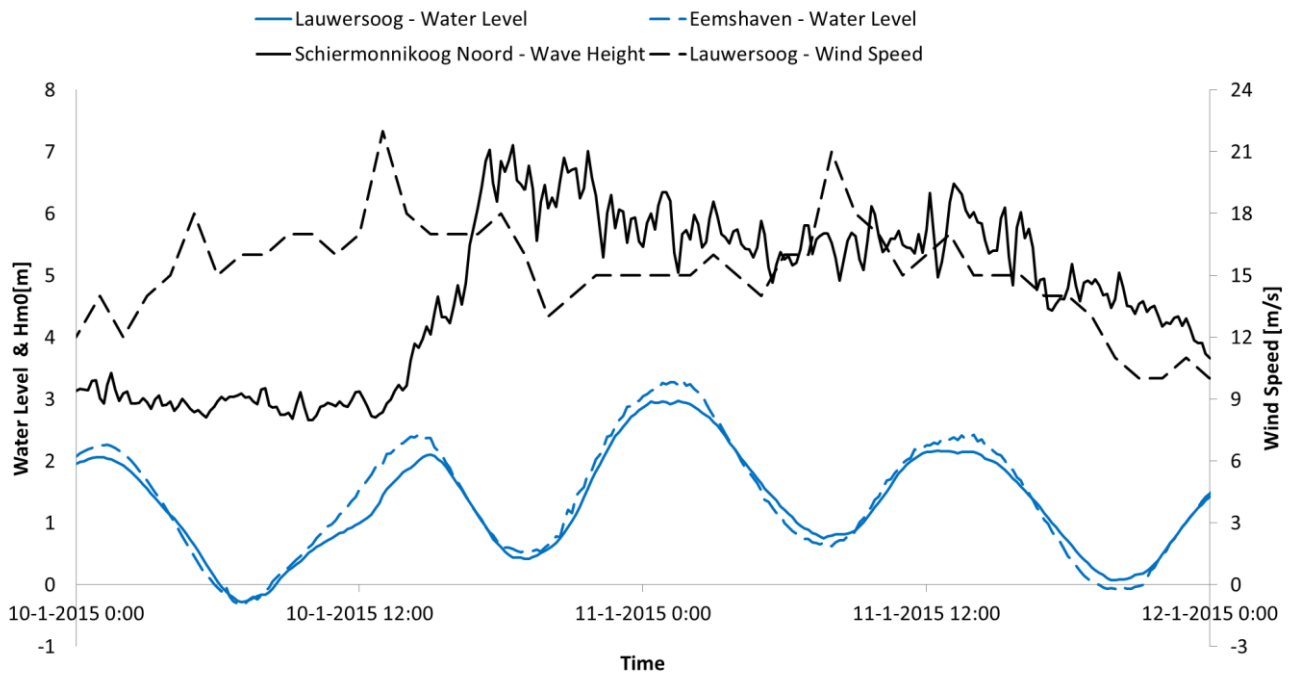


**Figure 5** The wave height and wind speed and water levels for in the eastern Wadden Sea

## 1.2. Problem statement

The studies performed in the field of wave-damping by vegetation can be brought back to two types of research. The first type of research is executed in a controlled environment such as a wave flume where the effects of different influences such as wave height, vegetation length and stem diameter can be isolated. These controlled environments do not reflect reality. The vegetation in these researches are either schematized using artificial vertical cylinders, flexible or rigid (Anderson & Smith, 2014), or a patch of uniform vegetation is harvested and is put into the flume.

The second type of research is performed in the field where the setup reflects realistic circumstances by definition and all parameters vary to some degree. However, the measurements are mostly taken during normal conditions when significant wave heights are below 0.2 m (Bradley & Houser, 2009; Lövstedt & Larson, 2010). To make the research relevant for engineers, it is important to have measurements during storm conditions to be able to extrapolate the effects of wave damping by vegetation towards design conditions.

This leads to the first problem statement which is that most studies are suited to support continued research into the subject but do not give the engineering community realistic examples of the impact of vegetation on wave damping during design conditions.

Secondly, the influence of the salt marshes in the Wadden Sea on the amount of wave-damping, and therefore safety, is currently unknown. Although it has been proven that vegetation results in wave-damping, the precise dissipation is unknown. This is very relevant information for local water boards since it helps them assess the importance of these areas.

Thirdly, it has not been achieved to replicate the flotsam levels accurately using a 2D model to this date (Smale, 2010). By achieving this, the flotsam levels could be used to calibrate wave models where little other information is known.

### **1.3. Objectives and research questions**

The objective of this research is to shed light on the influence that vegetated foreshores have on wave-damping, combined with the investigation whether it is possible to replicate the flotsam levels. This research adds to the limited knowledge about these areas so far. By investigating wave-damping by vegetation, this research can add to the implementation of this ecologically friendly solution to water safety issues. By attempting to replicate the flotsam levels, it is shown whether this source of information can be used reliably by water engineers in the future.

To shed light on the problems regarding the amount of wave-damping as a result of vegetated foreshores and the reproducibility of the flotsam levels, the following research questions are formulated.

- A. How do the salt marshes in the eastern Wadden Sea affect the wave conditions at the dike under design conditions?
- B. Can flotsam measurements serve as field evidence for wave run-up reduction by vegetated foreshores?
- C. Can flotsam measurements be approximated using a 2D wave model?

## **1.4. Methodology**

The research questions will be answered by following the steps described in this chapter.

### **Analysis of measurements**

The flotsam line was determined between Lauwersoog and Eemshaven. By comparing the flotsam height with the local bed level and extent of the vegetation, the influence of the foreshore characteristics on the maximum wave run-up can be determined. The pressure sensors measured the wave characteristics and water depth on and near the salt-marsh. By comparing the measurements from the different locations, the differences between the salt-marsh and the barren locations are found. This gives a second indication to the influence of the vegetated foreshore.

### **Build 1D and 2D model**

The 1D model is completely based on measurements taken on the salt marsh. The bed level is measured with an accurate GPS receiver and the wave conditions are determined with several pressure gauges. The 2D model is necessary due to the fact that not only the locations where wave measurements were taken can be investigated but also other locations on the salt marsh. This allows for investigation of the flotsam levels, making it a crucial part of this research. To make the comparison with the flotsam levels, it is important to take as much detail into account as possible for all forms of input.

### **Flotsam level reproduction**

The flotsam measurements are reproduced by determining the maximum wave run-up using the calibrated 2D model. The 2% wave run-up is determined using the method described by the Overtopping Manual (EurOtop, 2007) and explained in Chapter 1.2.2. The maximum wave run-up is then approximated from this value, which is compared to the measured flotsam levels in Chapter 5.

### **Scenario analysis 1D**

After building and calibrating the 1D model, it can be varied for different foreshore conditions such as changes in bottom height and amount of vegetation. The 1D model also allows for different methods to implement the vegetation. These two methods can then be compared.

### **Scenario analysis 2D**

A lot can be learnt about the influences of the salt marshes on wave-damping by introducing the design conditions for the dike section and varying the parameters and bathymetry for different scenarios. Conclusions can then be drawn about the effectiveness of the marshes

on wave-damping during design conditions and what the effect is when the salt marshes are changed.

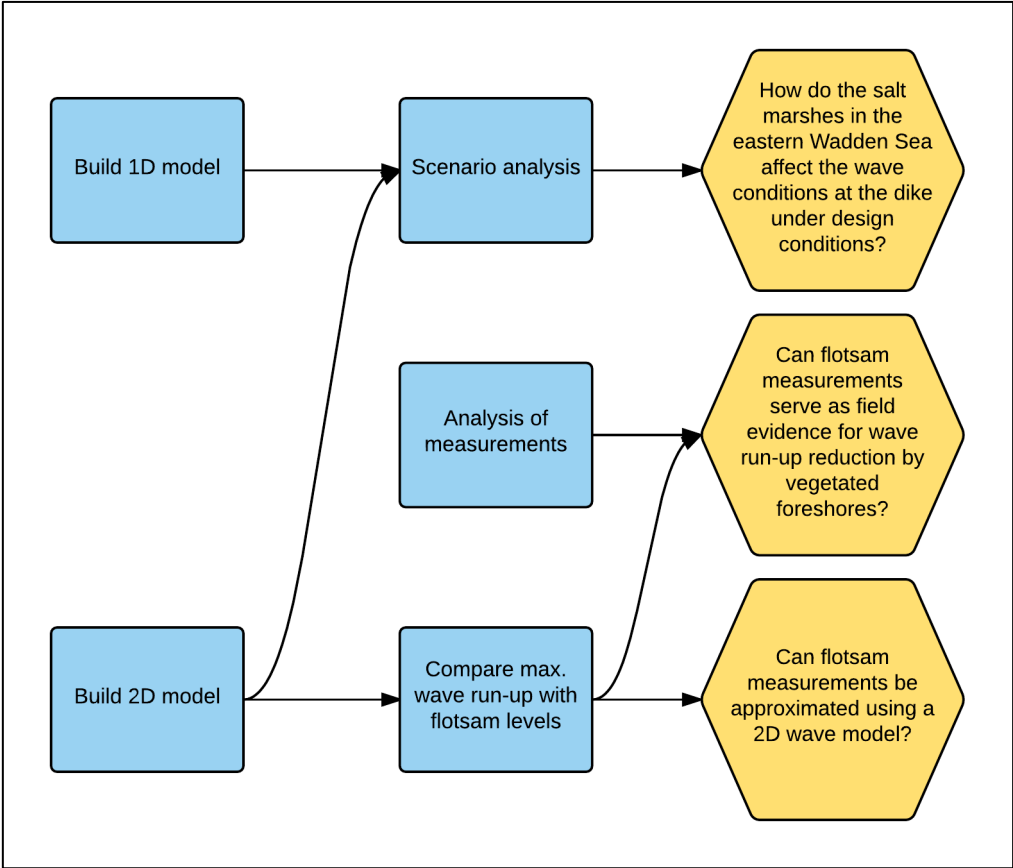


Figure 6 The steps taken in this research to answer all questions raised

## 2. Methods

In this chapter the different important methods which are used in this research are explained. First the two different models are introduced, with further details in the Chapter 4. Afterwards, the approach to calculate the maximum wave run-up to replicate flotsam levels is explained.

### 2.1. Modelling Setup

To answer the questions related to the reproduction of the flotsam levels and the influence of the foreshore vegetation, it is necessary to develop two models. By doing this, characteristics can be tested in both environments and compared. The first model, with an exploratory purpose, is made using SWAN in one dimension, also known as a line model. SWAN is a third generation wave model, which means that all relevant physical processes are explicitly represented by the different terms (such as: bed roughness, whitecapping and depth-induced wave breaking). Representing vegetation explicitly in the dissipation process is crucial for this research. This can be done in two different ways.

The first method increases the bottom roughness in order to increase dissipation (Hasselmann & Collins, 1968). The second method is aimed at realistically incorporating the vegetation into the model. By schematizing the vegetation as vertical cylinders with a certain length, diameter, number of stems and drag coefficient  $C_D$ . This second method was developed over the last few decades and was incorporated into SWAN (Mendez & Losada, 2004). The drag coefficient is dimensionless and is used in fluid dynamics to quantify the amount of drag, determined by the shape of the object.

The two methods to schematize the vegetation are investigated in 1D to see whether the different methods generate significantly different outcomes with respect to the capability of reproducing the  $H_{m0}$  values which were measured with the pressure sensors.

After calibration, the influence of different foreshore designs is investigated by scenario analysis for both the storm event and during a 1/10.000 storm event. The 1D model has the benefit that results can be calculated very fast. It takes only seconds to calculate the wave conditions, which is a large benefit compared to the 2D model which can take up to several days.

Delft3D is very suitable for the 2D model. This software package has been proven to be able to produce positive results in countless previous researches and is an established hydrodynamic modelling application. To answer the questions at hand, the two modules FLOW and WAVE are used. FLOW is designed to calculate hydrodynamic flows which leads to the necessary water levels and flow velocities. WAVE is a built-in version of SWAN

(Simulating WAVes Nearshore) which uses the information calculated by FLOW and can calculate the characteristics of the waves through the different source terms. Flow velocities are especially important for wave calculations in the shallow Wadden Sea since flow velocities can be significant (approximately 2 m/s) between high and low tide. These currents can have severe implications for the waves due to the exchange of energy which go from current to wave, and from wave to current. The version of SWAN which is currently implemented into WAVE is not capable of representing the vegetation as vertical cylinders. This means that in 2D, all vegetation is schematized as additional bed roughness.

### SWAN - 1D

The 1D model is located at the test site west of Eemshaven. The locations for sensors 1 to 5 situated perpendicularly to the dike are rebuilt in the model, represented by the white line in Figure 7.



Figure 7 1D model connects the sensors 1 to 5, the dike is on the right

The model is made up of several types of data (Figure 8). Firstly, the bathymetry is determined by measurements which were taken when the sensors were placed. Secondly, the wave characteristics and water level are found by analyzing the pressure sensors measurements. Thirdly, the wind velocity and direction are measured at the nearby weather station at Lauwersoog, coming from the west with a velocity of 15 m/s. Finally, the amount of bed roughness and vegetation drag which are needed cannot be measured but must be calibrated. This is shown in Chapter 4, including further details about the model.

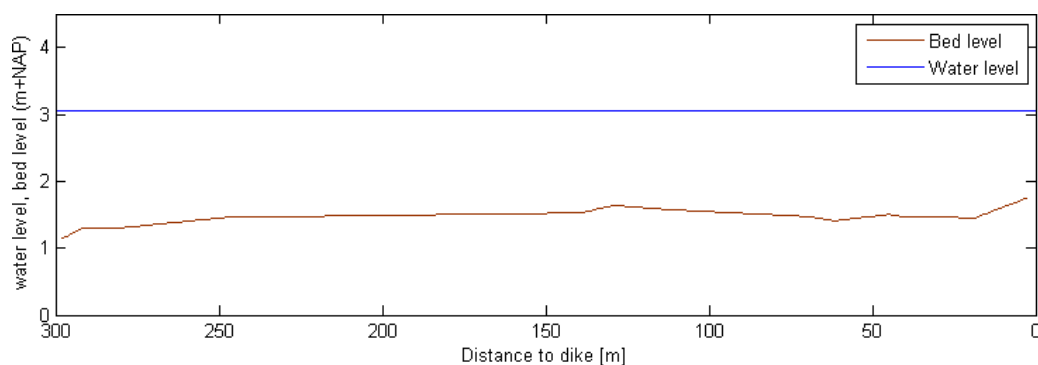
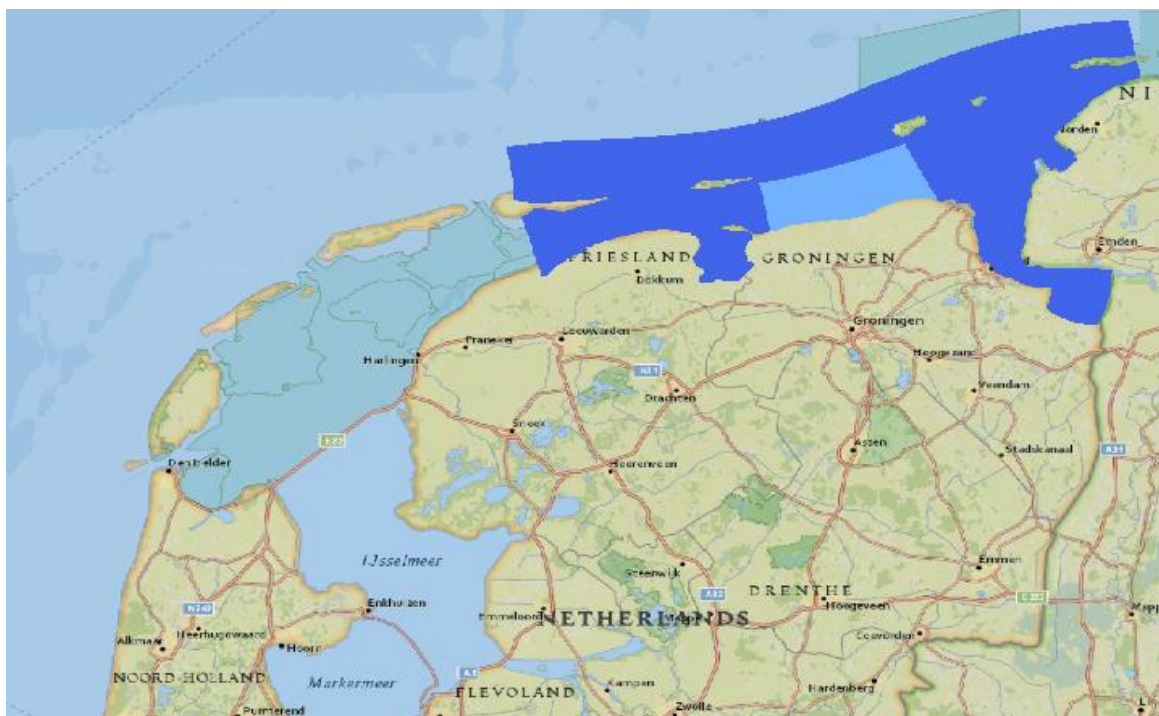


Figure 8 The 1D model during the peak of the storm

### Delft3D - 2D

The 2D model is a powerful tool due to the complexity that can be built into the model. By having this complexity, the real world situation can be represented more accurately and the confidence that can be put into the results is increased.

The 2D model grid is cut out of the large ZUNO model, replicating the grid used in a previous research (Smale, 2010) who developed a model to reproduce the flotsam levels for the storm of November 1<sup>st</sup> 2006. The area covered by the grid is approximately 110 km in alongshore direction and the center part of the model is approximately 20 km long in cross-shore direction (Figure 9). The locations for the western and eastern border of the model are chosen at the centers of the islands of Ameland and Norderney. The border therefore cuts through these islands, reducing the complexity of the flow patterns at the borders. The model has a grid size which varies in the model due to the fact that the grid is curvilinear. The coarse dark blue grid has a grid size of ~150 m in cross-shore direction and ~90 m alongshore. The refined light blue grid has a grid size of ~50 m by ~30 m. The cells in the refined area are 9 times smaller, 1:3 refinement in both directions.



**Figure 9** Grid used for the 2D model. The refined light blue grid is nested inside the larger dark blue grid

In previous research it was advised to maximize local variations in order to replicate the variations seen in the flotsam lines more successfully. To do this, the input for the model is spatially varied where possible. Wind and air pressure data from the HARMONIE model is used which varies hourly in time and space. The bathymetry (Figure 10) determined with the remote sensing technique known as lidar (collected by Actueel Hoogtebestand Nederland) is

used to have a high-quality foreshore bathymetry, supplemented by echo soundings by Rijkswaterstaat (vaklodingen) and the bed level found in the ZUNO model. The bed roughness varies in space in order to take the vegetated foreshores into account and is assumed constant for areas with no vegetation. For further details regarding the setup of the 2D model, parameter values and the different types of input, see Chapter 4.

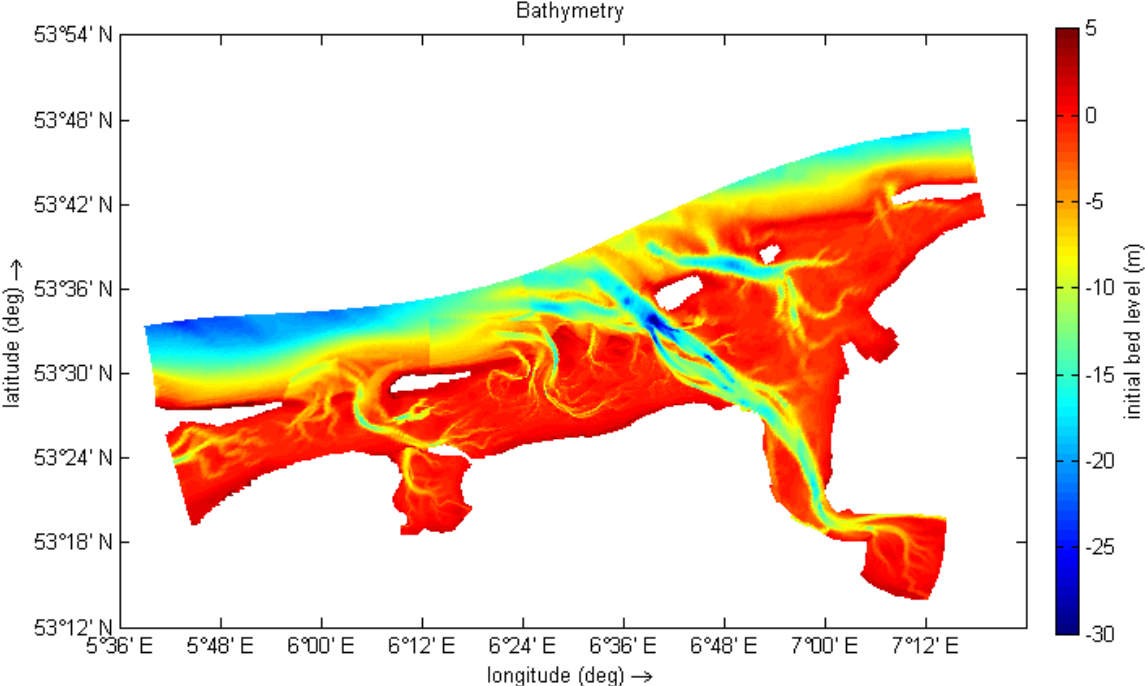


**Figure 10 Bathymetry, the combination of: lidar, echo soundings and ZUNO**

## 2.2. Wave run-up calculation

Since it is known that the flotsam is left on the slope by waves which run up the dike, a method is needed to determine the maximum run-up height which is achieved by waves locally (IJnsen, 1983).

The Overtopping Manual (EurOtop, 2007) is used to check whether dikes comply with the overtopping criteria. The basis of this calculation is the 2% run-up height,  $R_{u2\%}$  [m] (Figure 11). Calculating  $R_{u2\%}$  gives the height which is surpassed by 2% of all waves. To replicate the flotsam levels, it is necessary to translate  $R_{u2\%}$  to the maximum wave run-up,  $R_{max}$ .

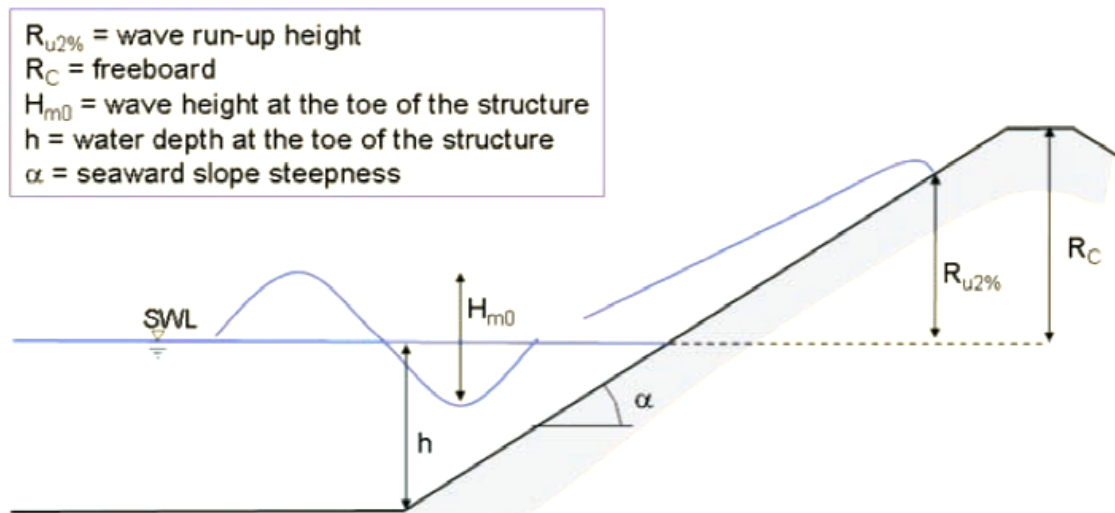


Figure 11 Important parameters to determine the 2% run-up (EurOtop, 2007)

### 2% wave run-up

The 2% wave run-up is influenced by several factors. Firstly, the significant wave height  $H_{m0}$  is dominant, found in both the equation for  $R_{u2\%}$  and the dimensionless breaker parameter  $\xi_{m-1,0}$  (Eq. 2).

The value for  $\xi_{m-1,0}$  is determined by  $H_{m0}$  and the deep water wave length  $L_{m-1,0}$  (Eq. 3). These values describe the wave steepness ( $H_{m0}/L_{m-1,0}$ ). For waves where the wave steepness is lower, the resulting run-up height is higher (EurOtop, 2007).  $\alpha$  is the slope of the dike in degrees, determined using detailed dike profile information from the water board Noorderzijlvest.

$$R_{u2\%} = 1.65H_{m0} * \gamma_b * \gamma_f * \gamma_\beta * \xi_{m-1,0} \quad \text{Eq. 1}$$

$$\xi_{m-1,0} = \tan \alpha / \sqrt{H_{m0}/L_{m-1,0}} \quad \text{Eq. 2}$$

$$L_{m-1,0} = gT_{m-1,0}^2 / 2\pi \quad \text{Eq. 3}$$

$\gamma_b$  is the berm influence factor [-]. Berms at the toe of the dike will result in lower run-up. However, in this research, no berms are present which means that  $\gamma_b = 1$  in all cases.

$\gamma_f$  is the slope roughness factor [-]. This factor takes the roughness of the dike slope revetment into account rock, which can be used to dissipate a part of the wave energy. In this research, all the dike profiles were made of smooth concrete which means that  $\gamma_f = 1$ .

$\gamma_\beta$  is the oblique wave attack factor [-]. This factor takes into account that waves will result in a lower run-up if they arrive at an angle to the normal of the dike. To determine this angle, both the orientation of the dike and the direction of the waves are needed. The dike orientation is determined locally using the detailed dike profile information supplied by the water board Noorderzijlvest. The wave direction is found using the 2D model. The angle of attack can then be determined ( $\beta$ ) and is used to calculate  $\gamma_\beta$  (Eq. 4).

$$\gamma_\beta = 1 - 0.0063|\beta| \quad \text{Eq. 4}$$

With  $\gamma_f$  and  $\gamma_b$  equal to 1, the run-up equation (Eq. 1) can be rewritten (Eq. 5) and it is seen that the run-up is determined by the slope of the dike  $\alpha$ , the wave characteristics  $H_{m0}$  and  $T_{m-1,0}$ , and the angle in degrees between the wave and normal of the dike  $\beta$ .

$$R_{u2\%} = 1.65H_{m0} * \tan \alpha / \sqrt{H_{m0} / \left( \frac{9.81T_{m-1,0}^2}{2\pi} \right)} * (1 - 0.0063|\beta|) \quad \text{Eq. 5}$$

### Maximum wave run-up

Between 1977 and 1983 a research was performed where the flotsam levels of 38 different storms were measured and used to create an approach of linking the 2% wave run-up to the maximum wave run-up,  $R_{u_{max}}$  (Ijnsen, 1983), assuming that the incoming waves had a Rayleigh distribution. This distribution describes the probability of wave heights based on the value for e.g.  $H_{m0}$  and assuming a certain shape (Figure 12).

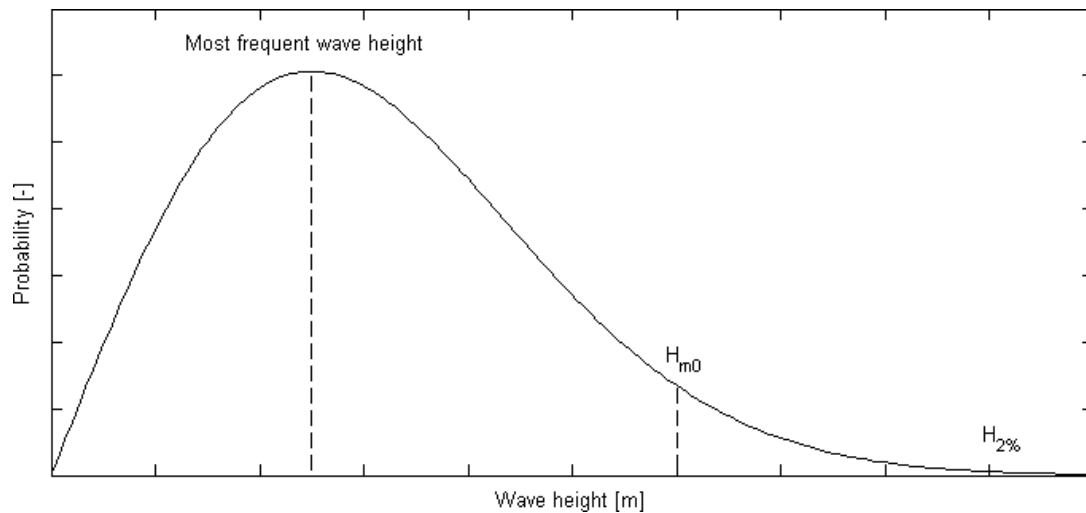


Figure 12 Rayleigh wave height distribution

Based on the Rayleigh distribution, Ijnsen states that the difference between  $R_{u_{max}}$  and  $R_{u_{2\%}}$  is approximately a factor 1.40, named  $\gamma_{max}$  [-] in this report (Eq. 6). Ijnsen found that the maximum wave run-up corresponded to the run-up related to the highest 0.3% of the waves.

$$R_{u_{max}} \approx \gamma_{max} * R_{u_{2\%}} \quad \text{Eq. 6}$$

In a later report, suggestions were made to lower the multiplication factor between  $R_{u_{max}}$  and  $R_{u_{2\%}}$  since a Rayleigh distribution is not valid in shallow water (de Reus, 1983). De Reus found that  $\gamma_{max}$  can range between 1.17 and 1.40.

The maximum wave run-up is added to the local water level  $\xi$  [m +NAP] to allow comparison with the flotsam levels.

## 3. Measurements

In order to assess the effects of the salt marshes on wave damping, local measurements were needed in addition to measurements available via Rijkswaterstaat. These were collected in preparation of this thesis on the coast of the eastern Wadden Sea. The test site location is introduced in the paragraph 3.1. The first type of measurements were performed using eight pressure gauges (3.2) located on and near the salt marsh which are used to determine the water depth and wave characteristics. The second type of measurements are the flotsam lines which were left after the storm. Flotsam lines consist of debris left on the slope of the dike which mark the highest wave run-up (see 3.3) and can therefore be used to compare the local wave conditions during the storm. The information found with the pressure gauges with respect to the waves and water depth is used to calibrate the models in Chapter 4. Both types of measurements are discussed and analyzed in this chapter.

### 3.1 Location

The Wadden Sea consists of an area enclosed by the coasts of the Netherlands, Germany, Denmark and the barrier islands. It is used by both humans and nature as it is an important area for migratory birds for which the area is a rich feeding ground. The area is mainly used by humans for gas-extractions, mud-hiking, sand, shell and salt mining. The Wadden Sea is mostly shallow with an average depth of only several meters during high tide. As a result, the area is an intertidal zone where the shallow areas flood and drain on a regular basis. This property is important for salt-marsh growth (Dijkema et al., 2007). Along the northeastern Dutch coast, man-made salt marshes make up large parts of the foreshore area.

The main location for this research lies on the coast of the eastern Wadden Sea, 10 kilometers west of Eemshaven (Figure 13, Figure 14). This part of the coastline has both types of foreshores that this research is concerned with. The vegetation on the salt marsh extends approximately 300 meters seaward and the area has a near-dike bed level of 1.6 meters +NAP. Areas without vegetation have a significantly lower bed level at approximately 0.7 meters +NAP. This means that the lower lying areas flood daily, while the vegetated areas generally only flood when there is water level set-up by wind.



Figure 13 Research location



Figure 14 Area of interest near Eemshaven, The Netherlands. Salt marshes seen on the left, sandy foreshore on the right and a transition zone in the center of the figure. The locations of the pressure gauges are shown by the icons.

### 3.2 Pressure gauges

Pressure gauges 1-5 were placed perpendicularly to the dike (Figure 15) over a length of 300 m in order to record the changes in the waves as they travel over the salt marsh. Gauges 5-8 were placed along the dike over a length of 1.5 km to record the differences in wave conditions near the dike between the vegetated areas (5, 6) and barren locations (7, 8).



**Figure 15** Locations of the pressure gauges



The waves and water level on the marsh were measured with pressure gauges which were dry during low tide and inundated during high tide. The pressure gauges had a certain height from the bottom which means that water depths below approximately 0.2 meters were not registered (Figure 16). These measurements can be seen in Figure 17.

$H_{m0}$  increases for increasing water depths and both the  $H_{m0}$  and water depth decrease for the pressure gauges closer to the dike due to the higher elevation of the bed.

**Figure 16** One of the pressure gauges used to determine water levels and wave characteristics on the marsh (Photo by: Vincent Vuik)

The sensors set up in a perpendicular pattern to the dike (sensors 1-5 in Figure 15), show that the water depth decreases for locations closer to the dike. The difference in water depth corresponds to the difference in bottom height (Figure 18), meaning that there was no significant wave-induced water level set-up. Values for  $H_{m0}$  decrease as the waves travel over the salt marsh from 0.77 to 0.36 m during the peak of the storm, a decrease of 0.41 meters or 53%.

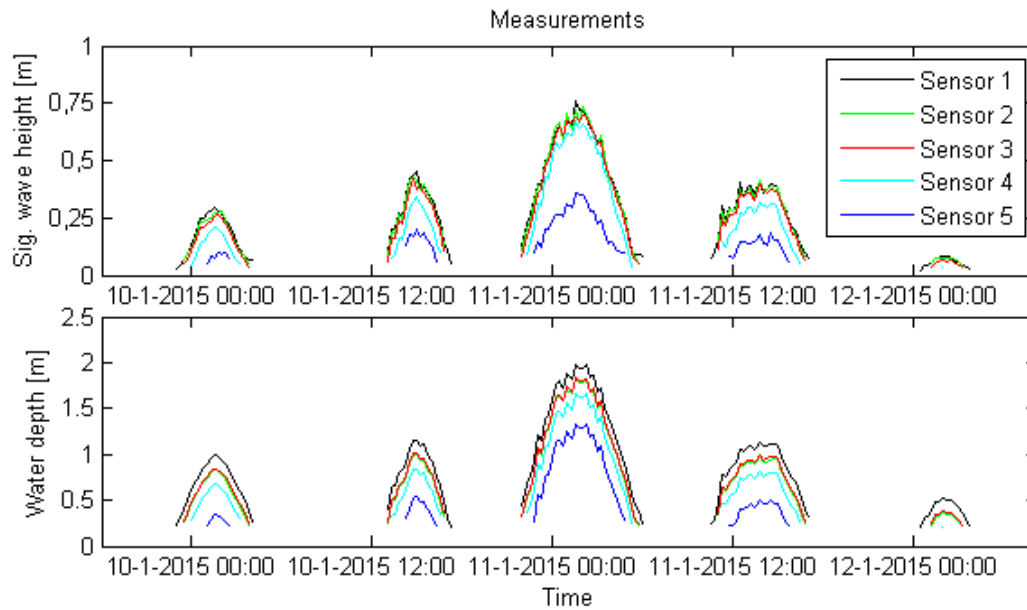


Figure 17 The measurements of sensors 1-5. Sensor 1 is outside the vegetated area and sensor 5 is near the dike

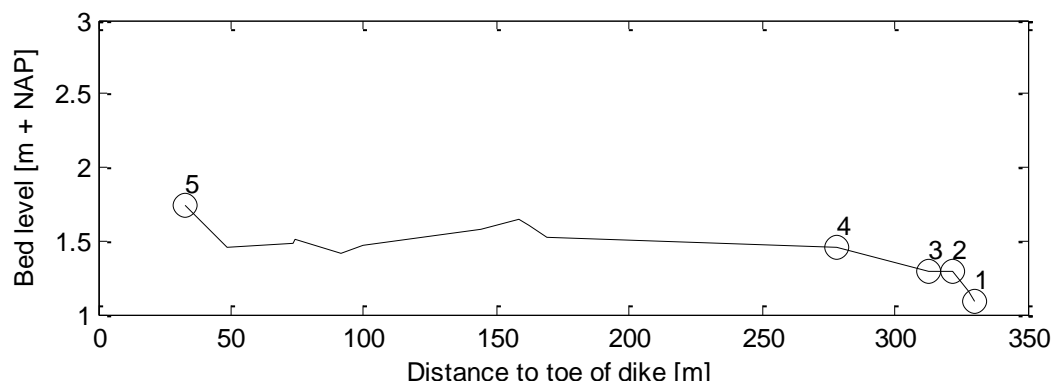
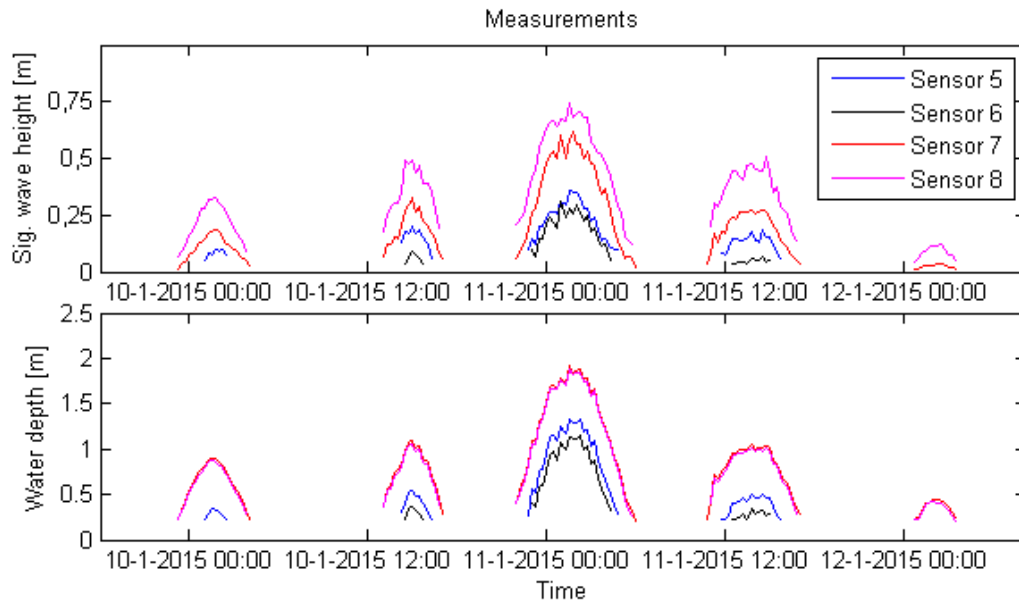
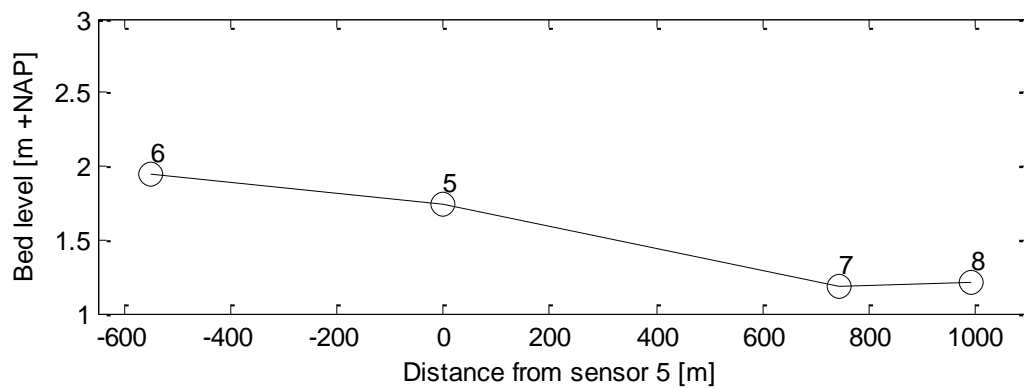


Figure 18 The pressure sensors perpendicular to the dike

The sensors 5-8 (Figure 19, Figure 20) were located at approximately equal distance from the dike but show very different wave conditions. For sensors 5 and 6 which are located in the vegetated area, the measured  $H_{m0}$  varied between 0.32 and 0.36 m which is a reduction of 51% compared to sensor 8 where vegetation was absent and the  $H_{m0}$  was 0.74 m. This difference is very similar to the difference found between the edge of the vegetation and near the dike, showing the influence of the presence of the salt marsh.



**Figure 19 Pressure gauge measurements. Sensor 5 and 6 are inside the vegetated area, the area of sensor 7 has some vegetation and sensor 8 is in a barren area**



**Figure 20 The pressure sensors along the dike**

### 3.3 Flotsam lines

Flotsam lines are the lines of debris left on a dike after a storm (Figure 3, Figure 21). In the case of the eastern Wadden Sea shoreline, the energy of the large waves on January 11<sup>th</sup> 2015 caused parts of the foreshore vegetation to be damaged. These particles were then transported by the waves and left on the dike, marking the highest wave run-up. In areas where there was little or no foreshore vegetation, the lines were significantly less visible. This means that in order to get clear flotsam lines, there has to be some type of buoyant material available in the area. Although the term flotsam *line* is used, it is not necessarily a clear and straight line (Figure 21). Subsequent lower waves also deposit flotsam on the dike, creating a band of flotsam. The height of the highest flotsam varies locally by approximately 2 meters horizontally or 0.4 meters vertically, an example of how this varies is given by the red arrow in the figure below.



Figure 21 Flotsam at the dike (Photo by: Vincent Vuik)

The flotsam level measurements were taken along the dike over a length of 33 km with most measurements taken in the study area on the eastern part, over a length of 14.5 km (Figure 22). The measured flotsam levels varied between 3.45 to 5.69 m +NAP. The height of the measurements vary in correspondence to the local extent of the foreshore vegetation (Figure 23).

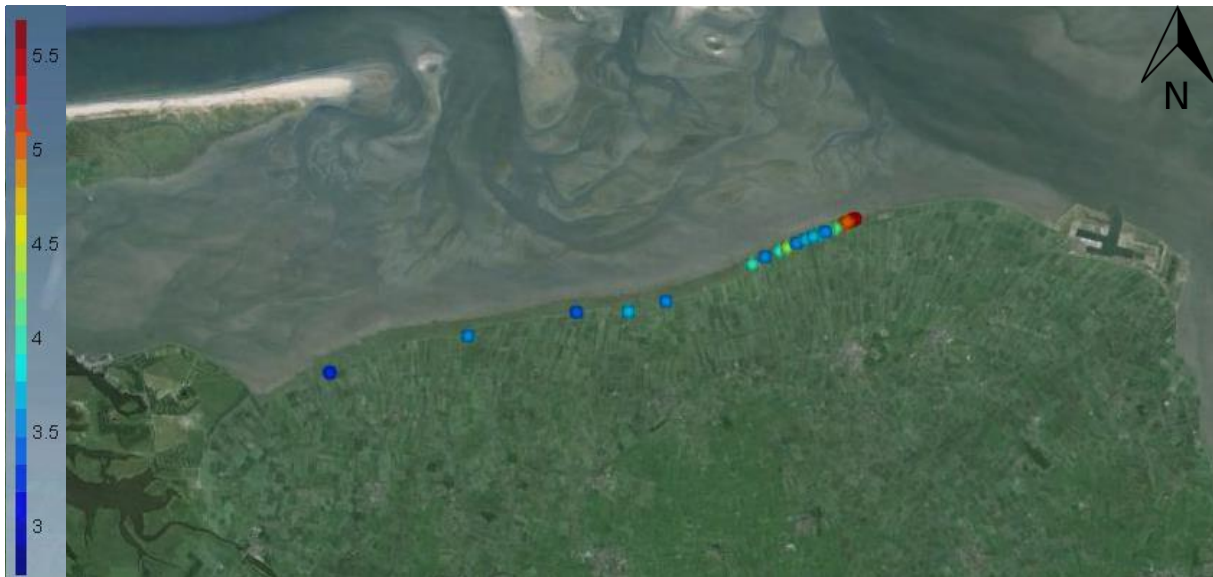


**Figure 22 Flotsam level point-measurements**



**Figure 23 The horizontal extent of the vegetation field (illustrated by the black line) and the flotsam level are related**

The flotsam lines are a valuable source of data, since the lines are a low-cost source of data that describe how the wave conditions varied along the coast. The flotsam levels show clear differences between locations where a vegetated foreshore was present and locations where the bed was lower and vegetation was absent (Figure 23). The flotsam measurements are compared to the extent of the vegetation field and the foreshore bed level (Figure 24).

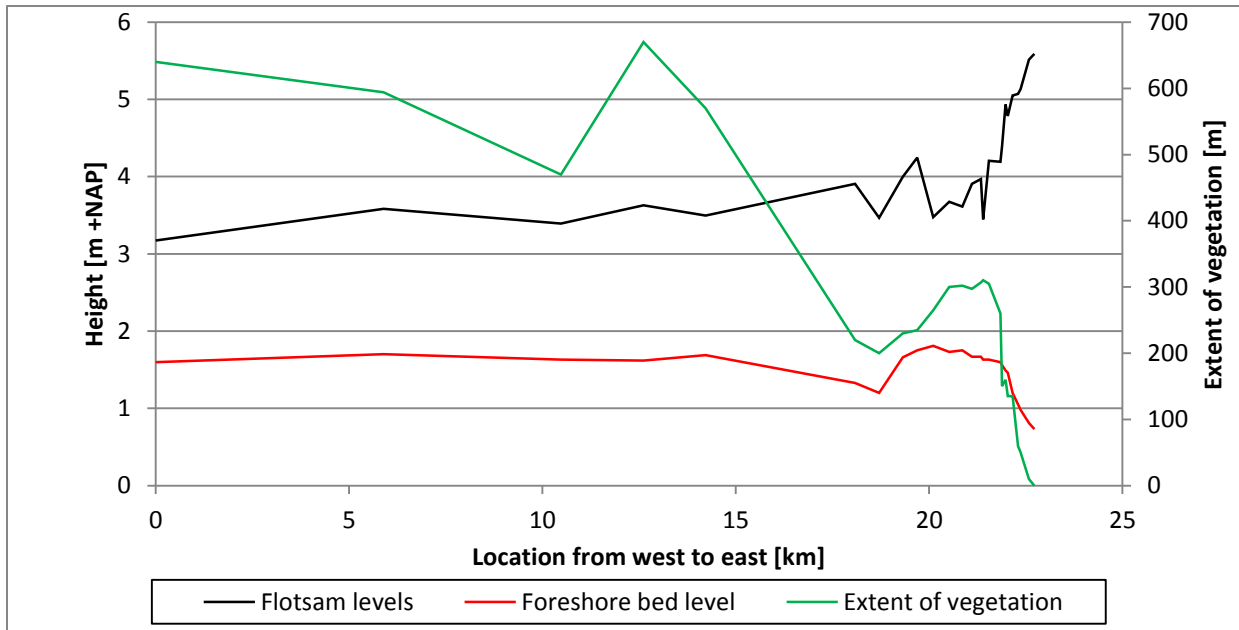


Figure 24 Flotsam measurements with the local conditions: extent of vegetation and foreshore bed level

The correlation between the three factors is high (Table 1, Figure 25). These correlation values clearly show the impact of the salt marshes. The probability that these values are not correlated is determined with the p-value (for N=25). This value is found to be smaller than 0.03% for the different correlations which means that the correlations presented in Table 1 are reliable. An extent of the vegetation field larger than 470 m did not lower the flotsam level further for the measured storm. The influence of the extent of the foreshore vegetation on the significant wave height at the toe of the dike is investigated for design conditions in Chapter 6.3.

Table 1 Correlation between the three parameters

	<i>Flotsam level</i>	<i>Foreshore depth</i>	<i>Extent of vegetation</i>
<i>Flotsam level</i>	-	-0.78	-0.80
<i>Foreshore depth</i>	-0.78	-	0.66
<i>Extent of vegetation</i>	-0.80	0.66	-

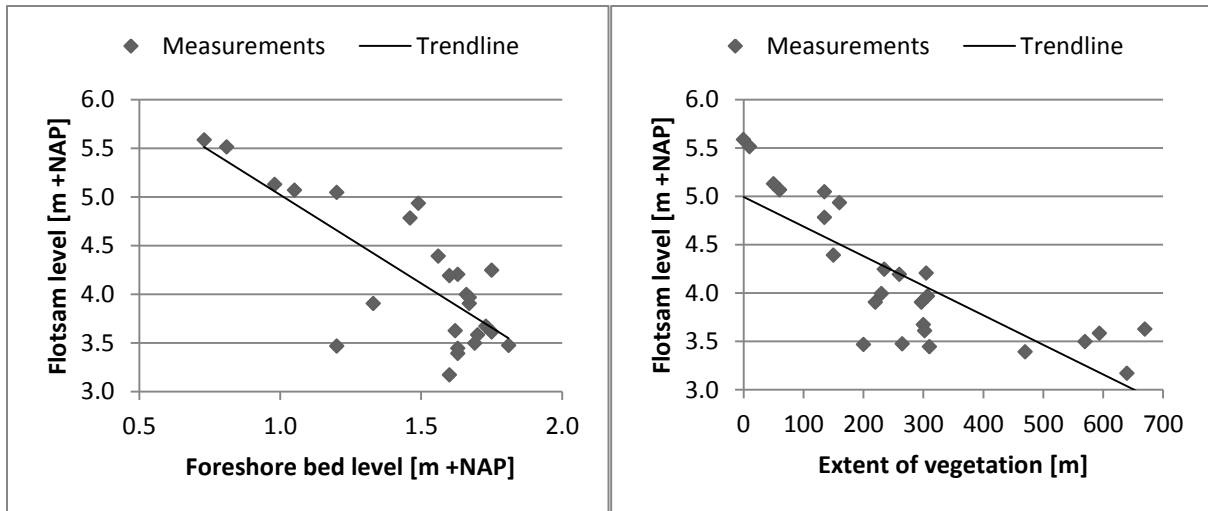


Figure 25 The flotsam level as a function of the foreshore bed level (left) and the extent of the vegetation (right) and the trendlines represent the correlation

### 3.4 Summary

The flotsam level is highly influenced by the foreshore conditions which is shown both by the figures and by the high correlation values. The difference in flotsam level was up to 2.00 m for vegetated compared to non-vegetated areas, which is a significant reduction of the maximum wave run-up height during storms. It can be ruled out that water level differences (due to wind- or wave-induced set-up) were of significant influence for the differences for the locations near the pressure sensors, since the water level differences were  $\leq 5$  cm.

The length of the vegetation field and the foreshore bed level are positively correlated, which can be explained by the fact that this type of vegetation (BRON) is only possible on intertidal areas. The salt marshes need to be generally dry but flood regularly. To achieve this, the bed needs to exceed a certain critical level. Sedimentation is then increased and erosion is reduced due to the presence of the vegetation.

The wave height measurements reveal that waves traveling over the vegetated area, which had a length of 300 m, were dissipated by 0.41 m or 53%. Waves that did not travel over the shallow vegetated area, arrived practically undampened at 0.71 m. This means that the full difference in wave height is caused by the presence, or lack of, the salt marshes.

## 4. Models

This chapter gives a detailed description of the two models which are used in this research. Both models were introduced in Chapter 2.1.

### 4.1. 1D model

The input required for the 1D model consists of the bathymetry along the length of the model, the water level, wind speed, wind direction, wave characteristics for at least two points along the model and the vegetation density along the length of the model. The bottom roughness is an important source of dissipation. However, this is difficult to measure which means that it has to be estimated. Even though the vegetation density is measured at one location and can be related to other locations to have a full map of the vegetation density, the methods available to calculate the drag coefficient from this data seem not to be accurate outside controlled experiments (Fischenich & Dudley, 1999; Hu, Stive, & Zitman, 2012). Therefore, the vegetation drag coefficient is the second unknown parameter.

The setup of the model is visualized in Figure 26. The bed level is completely determined by measurements taken locally using an accurate GPS device. It can be seen that the vegetation is found almost everywhere along the salt-marsh, however, vegetation density does vary. The vegetation is generally more dense, taller and healthier on the right side of Figure 26 (location of the dike). This turns into pioneer vegetation towards the left side (edge of the marsh), which is generally shorter, less dense and damaged by waves (Figure 27).

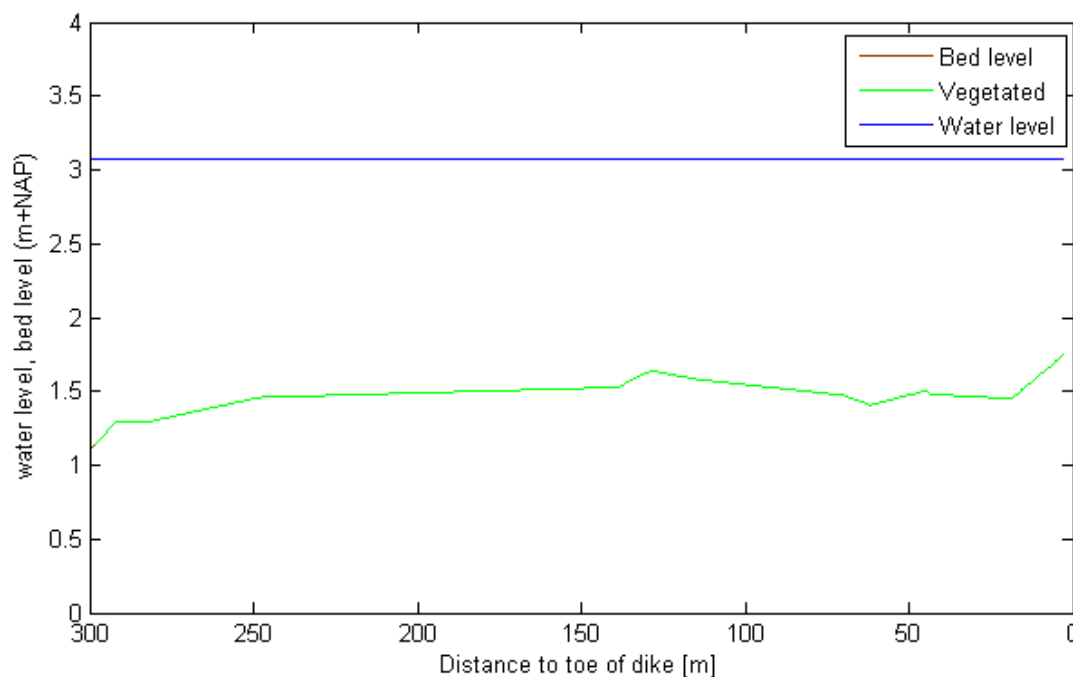


**Figure 26** Bed level, vegetated area and water level during the peak of the storm. Vegetation completely covers the bed except for the left-most part.

The waves coming in from just outside the edge of the salt-marsh (sensor 1) serve as input for the model. These waves then travel over the marsh. The wave height near the dike is then compared to the measurement for this location (sensor 5). The wave measurements were discussed in Chapter 3.2.



**Figure 27 Difference in vegetation, Left: Healthy near-dike vegetation, Right: pioneer vegetation near the edge of the marsh (Photos by: Vincent Vuik)**

## Settings

There are five different source terms in the 1D model that need estimation or calibration.

### ***Depth-induced wave breaking***

Firstly the depth-induced wave breaking can be determined from literature. Although opinions differ on the right value, in 1993 it was found that the dimensionless breaker index ( $\gamma$ ) averaged 0.79, this value was the average found after a large number of experiments (Kaminsky & Kraus, 1993).

### ***Wave-wave interaction***

Secondly, wave-wave interactions can be divided into quadruplet and trilinear interactions. Both redistribute energy along the spectrum, mainly from the peak to lower and higher frequencies. Quadruplet interactions are not applied for this case since this is an effect that only occurs in deep water. Trilinear interactions are relevant for shallow water depths but it was found to have no significant effect in this one-dimensional case. This is most likely caused by the short length of the model which is about 300 meters. The  $H_{m0}$  is not influenced since is defined as the height which is surpassed by 1/3 of the waves, so even though the shape of the spectrum changes slightly, the 1/3 highest waves remain roughly the same.

### ***Whitecapping***

Thirdly, even though the wind velocity was on average approximately 16 m/s, since the wind came from the west (on average directed from 272°), the wind was found to have little effect in sustaining the wave-height and dissipation by white-capping was limited.

### ***Bed friction***

The dissipation by bed friction  $S_{ds,b}$  (Eq. 7) can be schematized in SWAN using three different methods to determine the bottom friction coefficient  $C_b$  but all use the following equation.

$$S_{ds,b} = -C_b \frac{\sigma^2}{g^2 \sinh^2 kh} E(\sigma, \theta) \quad \text{Eq. 7}$$

With,

$E(\sigma, \theta)$	wave variance spectrum	[J m <sup>-2</sup> ]
$\sigma$	wave frequency	[s <sup>-1</sup> ]
$\theta$	wave direction	[rad]
$k$	wave number ( $2\pi/\lambda$ )	[m <sup>-1</sup> ]
$h$	water depth	[m]

The first method is the empirical model of JONSWAP where  $C_b$  is defined as a dimensionless constant (Hasselmann et al., 1973). The second approach is the drag law model of Collins where  $C_b$  is dependent on the bottom orbital motion  $U_{rms}$  and a non-dimensional friction factor  $C_f$  (Collins, 1972). The third approach is the eddy-viscosity model (Madsen, Poon, & Graber, 1988), which is similar to the drag law model of Collins but where the non-dimensional friction factor (called  $f_w$  instead of  $C_f$ ) itself depends on the bottom roughness length  $K_N$  [m] and a representative near-bottom excursion amplitude  $a_b$ . For shallow areas it is advised to use the method of Madsen since it takes changing wave conditions into account through the value for  $a_b$  (Padilla-Hernández & Monbaliu, 2001).  $K_N$  is varied for calibration purposes.

### **Vegetation drag**

The dissipation by vegetation  $S_{ds,veg}$  (Eq. 8) depends on several parameters which are spatially varying, determined through literature, photos and a measurement. The vegetation module in SWAN calculates the dissipation with the following expression. Using this approach, the vegetation is schematized as vertical cylinders (Figure 28).

$$S_{ds,veg} = - \sqrt{\frac{2}{\pi}} g^2 C_D b_v N_v \left(\frac{k}{\sigma}\right)^3 \frac{\sinh^3 kah + 3\sinh kah}{3k \cosh^3 kh} \sqrt{E_{tot}} E(\sigma, \theta) \quad \text{Eq. 8}$$

With,

$C_D$	drag factor	[-]
$b$	stem diameter	[m]
$N$	number of stems	[-]
$\alpha h$	vegetation height	[m]
$E_{tot}$	total wave energy	[J m <sup>-2</sup> ]

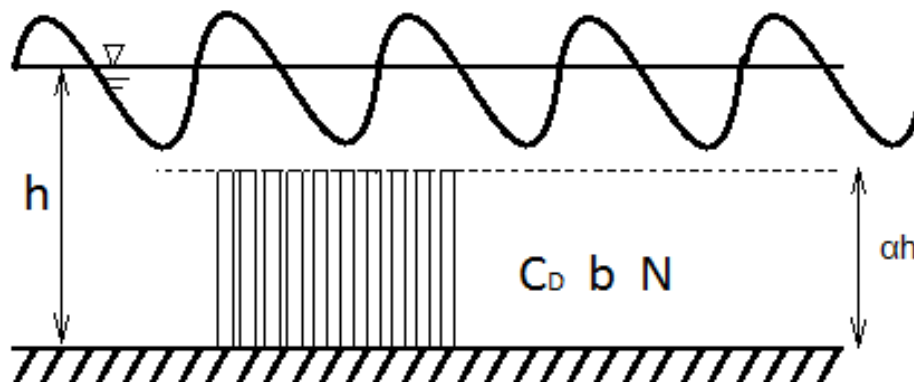


Figure 28 Vegetation is schematized as vertical cylinders with a certain height  $ah$ , drag  $C_D$ , diameter ( $b$ ) and number per square meter ( $N$ )

A measurement was performed which found the dry biomass for an area of 25x25 centimeters (Figure 29). The dry biomass taken near sensor 4 was weighed and extrapolated to 732 grams per  $m^2$ . The height and diameter were estimated from photos. The volume per stem then follows from the formula to determine the volume of a cylinder ( $V_c = 0.25 h\pi D^2$ ). To compensate for the facts that the vegetation is not uniform due to the ditches in the salt-marsh, which are in place for drainage purposes, and that vegetation is absent in places, the dry biomass is lowered by 10% for sensor 5 and 20% for sensor 4. The dry biomass for sensors 1-3 are estimated as a percentage of the measurement using photos. The dry biomass for sensors 1,2 and 3 is reduced by, respectively, 97, 95 and 50%. The biomass is not reduced further as is done for sensors 4 and 5, due to the high uncertainty in the estimations themselves.

The wet biomass of the vegetation is estimated by multiplying the dry biomass with a factor  $0.85^{-1}$ , which is a realistic value for similar types of vegetation (Butler et al., 2006). Finally, using a wet volumetric density of  $769 \text{ kg m}^{-3}$  (Walker, 2014), the volume per  $m^2$  and the number of stems per  $m^2$  are found.

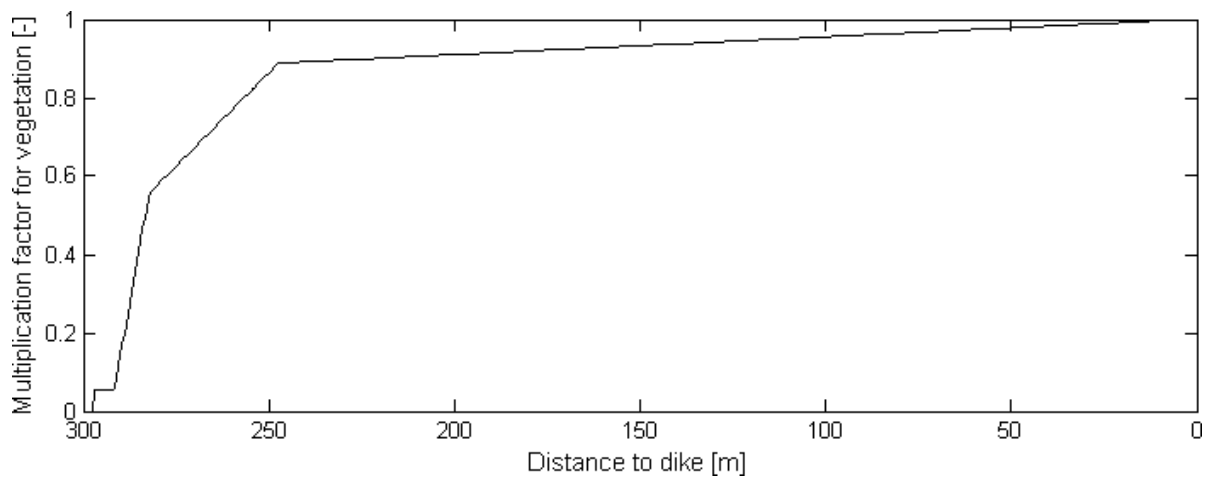
The variation in vegetation is implemented in the 1D SWAN model by linear interpolation between these points (see Figure 30 for the final result).

Table 2 Vegetation characteristics determined for the five sensors

	Height [m]	Diameter [mm]	Volume per stem [ $m^3$ ]	Dry biomass [ $g/m^2$ ]	Wet biomass [ $g/m^2$ ]	Volume per $m^2$ [ $m^3$ ]	# stems
<i>Sensor1</i>	0.05	3	3.53E-07	18.3	21.5	2.80E-05	79
<i>Sensor2</i>	0.1	3	7.07E-07	36.6	43.1	5.60E-05	79
<i>Sensor3</i>	0.1	3	7.07E-07	366.3	431.0	5.60E-04	793
<i>Sensor4</i>	0.4	3	2.83E-06	586.1	689.5	8.97E-04	317
<i>Sensor5</i>	0.4	3	2.83E-06	659.4	775.7	1.01E-03	357



**Figure 29 Biomass measurement (Photo by: Vincent Vuik)**



**Figure 30 The spatially varying vegetation factor (NPLANTS) which is used to represent the differences in vegetation density over the salt-marsh**

### **Calibration**

The one-dimensional SWAN model is calibrated for two situations. Firstly, calibration is performed for the situation stated in the previous paragraph where vegetation is schematized as rigid vertical cylinders. By varying the drag coefficient  $C_D$  over a realistic range of 0 and 1, the best fit with the measurements can be determined. Secondly, the vegetation is schematized as additional bed roughness via the parameter  $K_N$ . Although this seems like a simplification of the vegetation wave-damping processes, it is a realistic representation when the length of the vegetation is small compared to the water depth.

Calibration was performed for the peak of the storm which lasted from approximately 22:30 on the 10<sup>th</sup> of January to 4:30 on the 11<sup>th</sup>. The model is later validated for the pre- and after-storm peaks (Figure 31).

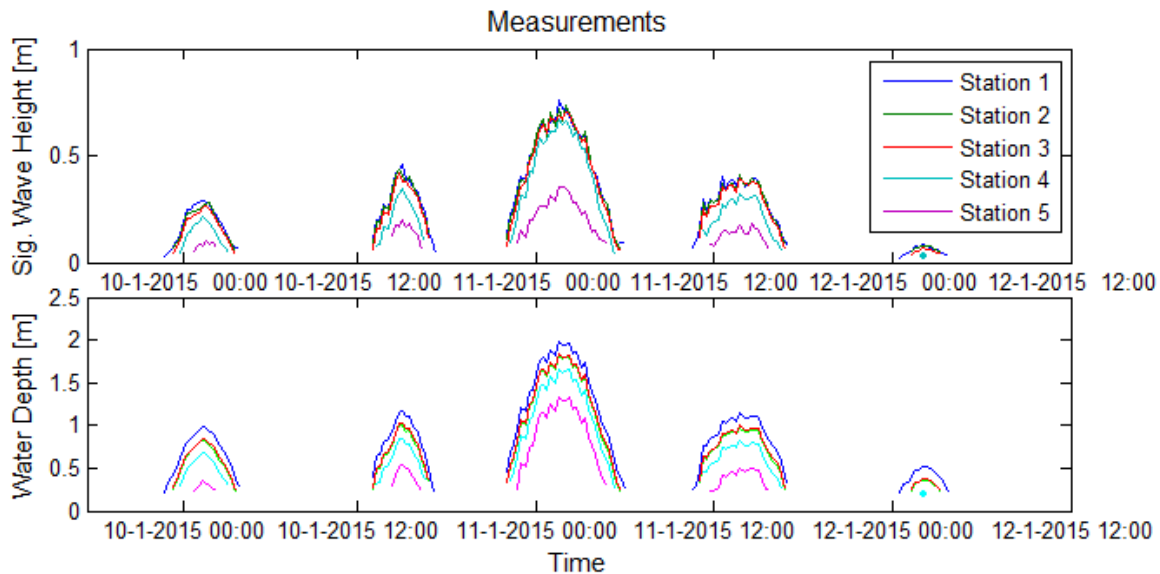
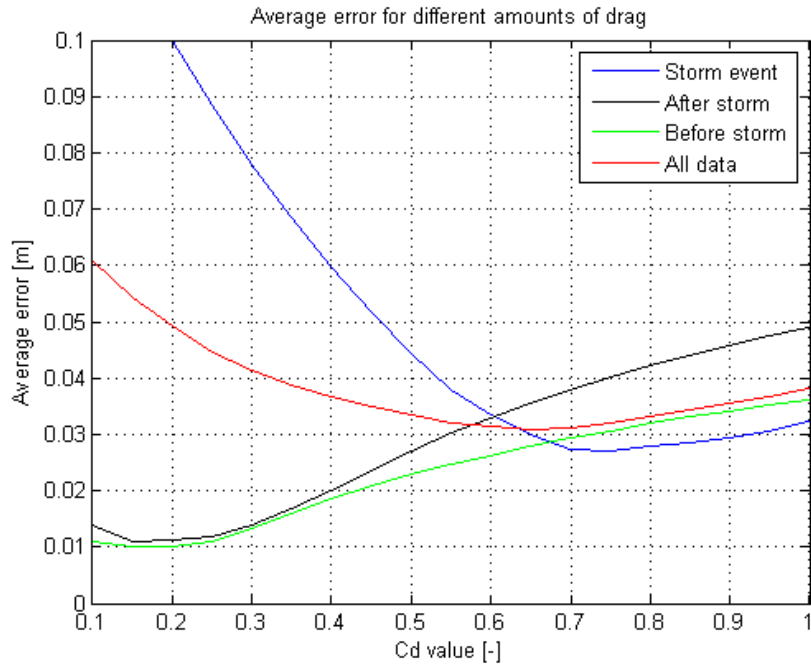


Figure 31 Waves measured during the storm, sensor 1 is outside the vegetated area and sensor 5 is near the dike

### *Calibration for the drag coefficient*

The bottom roughness length scale  $K_N$  is assumed to be 0.01 m, which is the same as was found in other regions in the Wadden Sea (Donker, 2015). The drag coefficient for  $C_D$  is then varied between 0 and 1 and the results are compared.

By comparing the average error for each run and the wave heights for the three largest peaks, it is found that the model is accurate at reproducing the storm conditions with an average error of 2.7 centimeters for the 25 7-minute intervals during the peak of the storm for  $C_D = 0.65$  (Figure 32). This can also be seen in Figure 33 where the wave height for the storm event is reproduced accurately and the before- and after-storm events are inaccurate. This is not solved by changing the drag coefficient to the optimum for the measurements for the three highest peaks where  $C_D = 0.55$  (Figure 34), nor when the drag coefficient  $C_D$  is set to the 0.1 to reflect the optimum for the before- and after-storm events (Figure 35).



**Figure 32 Average error for different drag coefficient values**

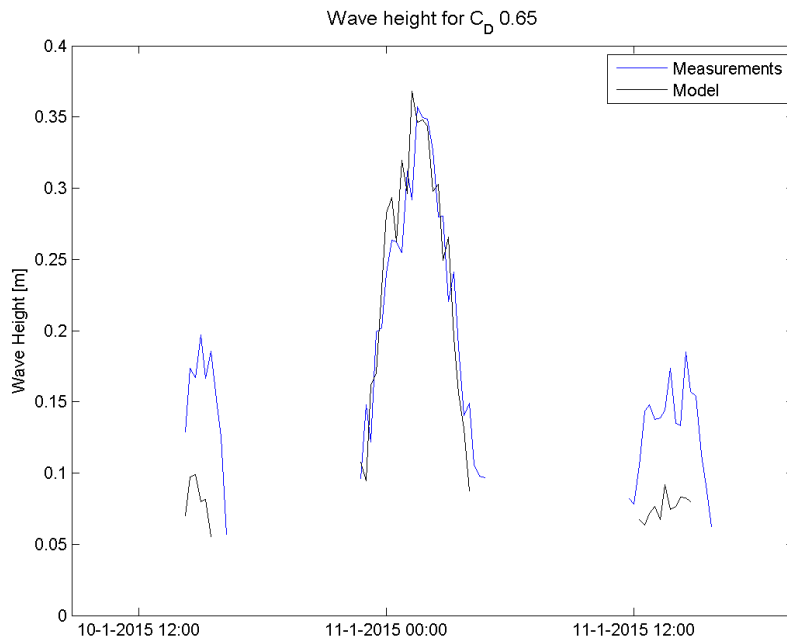


**Figure 33 Measured significant wave height versus the model outcome for  $C_D = 0.65$  at the near-dike sensor 5**

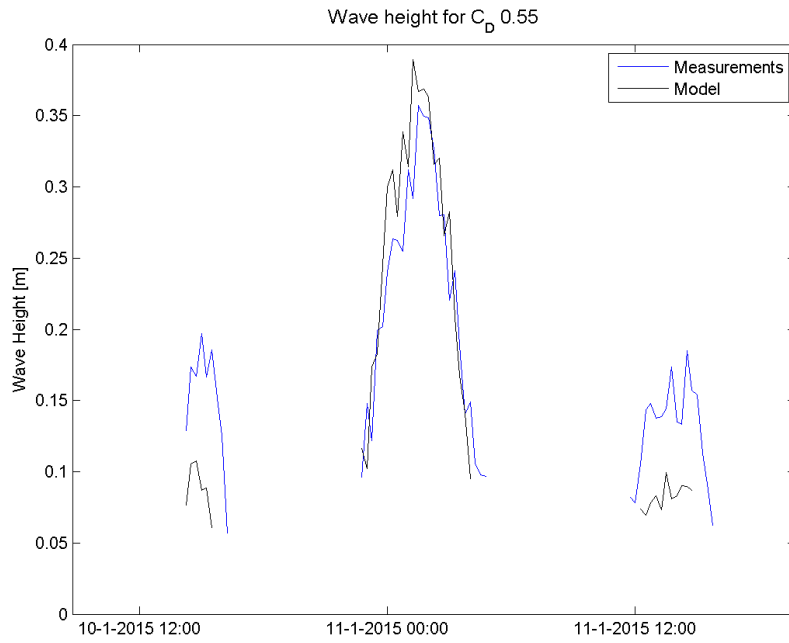


Figure 34 Measured significant wave height versus the model outcome for  $C_D = 0.55$

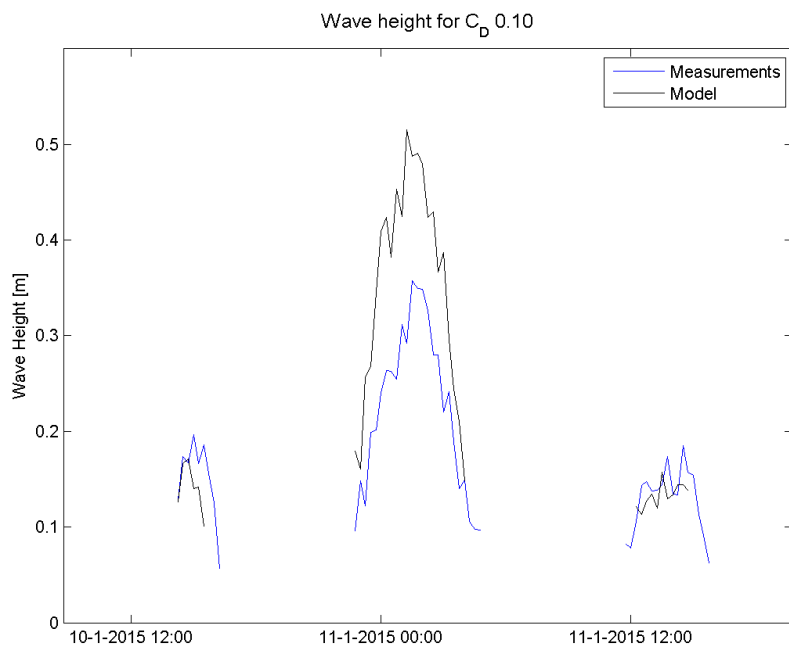
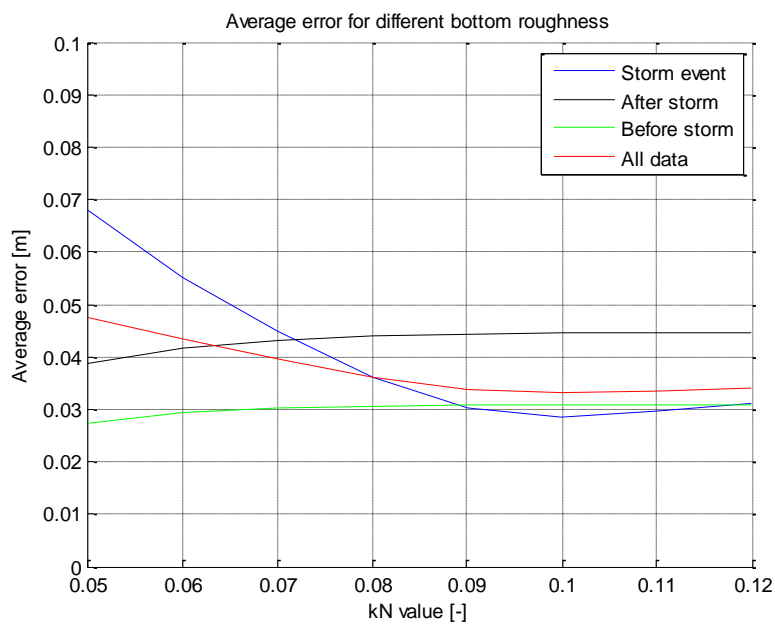


Figure 35 Measured significant wave versus the model outcome for  $C_D = 0.10$

### ***Calibration for the bottom roughness length***

The 1D model will now be calibrated for the bottom roughness length  $K_N$ . A separate schematization of the vegetation is now left out. The dissipation as a result of the vegetation will now be compensated for by an increased  $K_N$  value. When the  $K_N$  value is varied from 0.05 to 0.12 meters, the following average error is found (Figure 36).

This result is very similar to what was found when varying  $C_D$ , meaning that the model works equally well at reproducing the measurements for both schematizations. The before- and after-storm events show significant underestimation of the wave heights. This could be caused by the lower water levels which increases dissipation.



**Figure 36 Average error for different bottom roughness length scale values**

## 4.2. 2D model

The next several paragraphs present the different types of input and settings used to build the 2D model. The performance of the model is shown at the end of this chapter. The different types of input are the bathymetry, wind and atmospheric pressure, flow boundary conditions and wave boundary conditions. The 2D model was introduced in Chapter 2.1.

### Bathymetry

The bathymetry (Figure 37) consists of input from three sources which are layered according to the expected accuracy. Firstly, with the highest priority, the lidar data. This is widely used, freely available and known for its high accuracy. This data is collected using flyovers with laser reflection technology and is later checked and edited before the data is published in order to remove inaccuracies.

The second bathymetry source are the echo soundings known as “vaklodingen”. These are collected by survey ships which can measure the bathymetry by measuring the reflected sound waves. The drawback of this method is that the measurements can only be performed when the water depth is sufficient. On the salt marshes, where the water depth is generally zero except during storms, this technique cannot be used. However, these measurements are accurate in the order of several centimeters for areas where measurements are possible (Cronin & Bing Wang, 2012). One problem is that the measurements are collected over many years. This means that for the area which is covered by the grid, contains measurements dating back up to 15 years are combined with new measurements. Due to the dynamic nature of the Wadden Sea, troughs have meandered in the time between two measurements. Two cells which are connected can therefore have very different water depths, resulting in local inaccuracies regarding flow velocity and direction. This did not lead to issues for this research since the storm caused increased water levels which reduces this phenomena.

The final bathymetry source is the ZUNO (Southern North Sea) model. This WAQUA model, created by Rijkswaterstaat, is used to determine water levels along the entire Dutch coast. Since ZUNO covers the entire domain of the model, any missing depths are filled in from this source. The accuracy of this data is low due to the large grid cells in ZUNO.

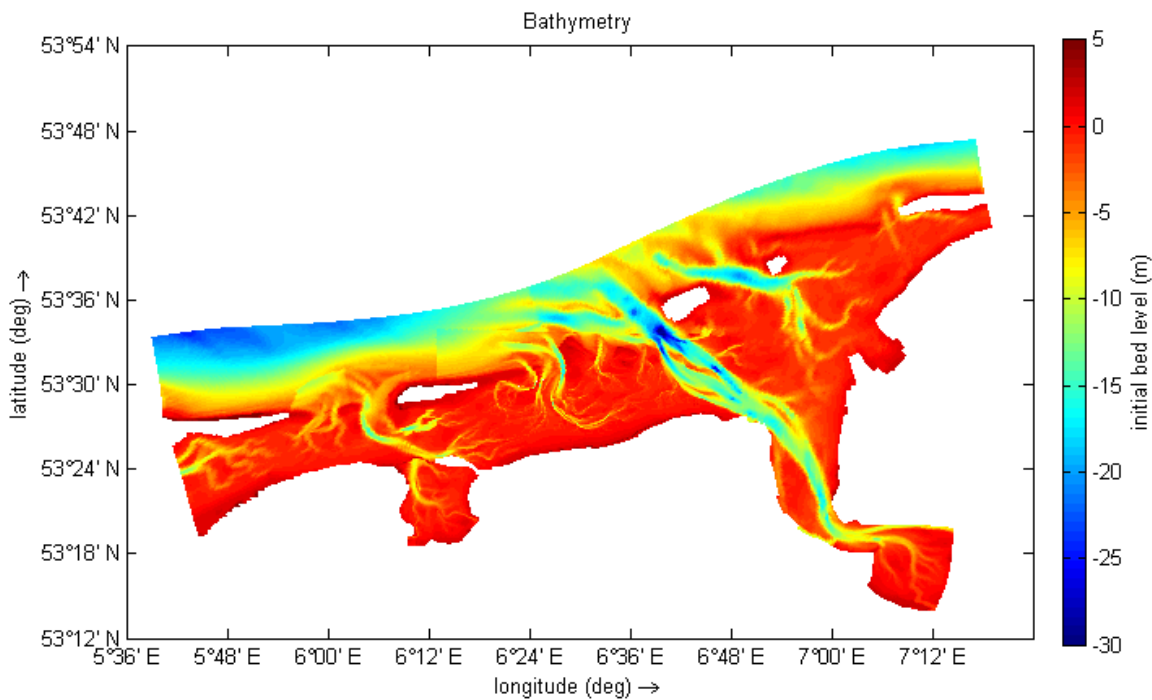


**Figure 37 Bathymetry, a combination of: lidar, echo soundings and the ZUNO bed level**

### **Wind and air pressure**

By allowing the wind and air pressure input vary spatially, the local variability of the model is increased. The results of the HARMONIE atmospheric model are used to generate a grid which fits over the 2D model. This grid has a resolution of 2.5 by 2.5 kilometer, matching the HARMONIE model. An example of the similar but larger HIRLAM model is shown in Figure 4 in Chapter 1.1.1.1. During the peak of the storm at January 11<sup>th</sup>, the wind speeds were approximately 20-25 m/s in southeastern direction.

Air pressure differences result in water transport from high to low pressure areas. In the large oceans the differences in air pressure can lead to changes in water level up to several tens of centimeters. On the scale of this model the effect is limited due to the small differences in air pressure. However, to increase the amount of realistic data put into the model, it is included. The air pressure varies from 1008 to 1009 mbar.

### **Flow boundary conditions**

The FLOW module is used to calculate a spatially varying water depth and flow velocities in the eastern Wadden Sea. The boundary conditions for this module (Figure 38) consist of water levels along the northern boundary and flow velocities along the western and eastern boundaries. These values are taken from the larger ZUNO model (Figure 39) which connects seamlessly to the grid and has 1 cell for every 3 cells in the 2D model. Therefore, all boundary conditions are given per 3 cells (Figure 40).



**Figure 38** Flow boundary locations. The northern (red) boundary dictate a water level, green boundaries dictate flow in and out of the boundary. The missing square is filled by the refined grid.

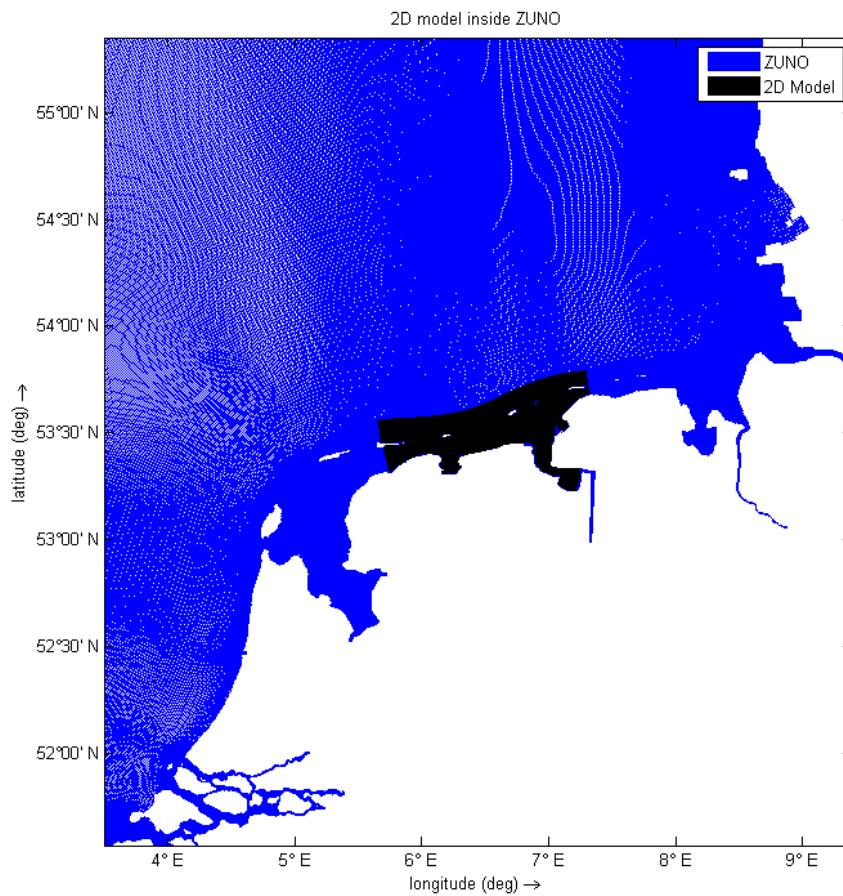


**Figure 39** The 2D Wadden Sea model inside the larger ZUNO model

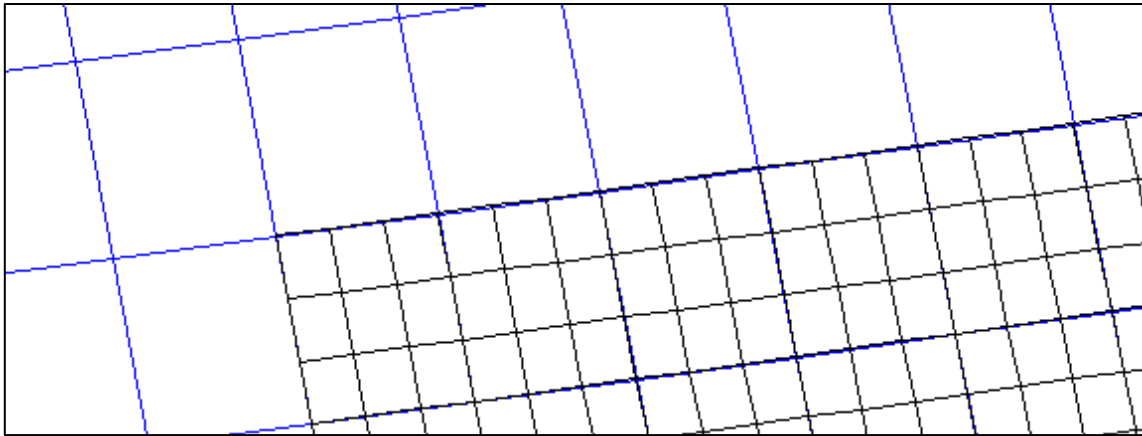


Figure 40 Northwestern connection between ZUNO and the 2D Wadden Sea model. Refinement is 1:3

### Wave boundary conditions

The boundary conditions for the WAVE module in Delft3D is taken from buoy measurements. There are several locations in and near the Wadden Sea that register the wave height, wave period, mean wave direction, etc. The most relevant for this model is buoy WEW1 (Figure 41), just north-east of Schiermonnikoog and is located in line with the salt marshes. The wave conditions at this location is the most influential for the salt marshes. It is not possible to let the wave conditions on northern boundary vary through linear interpolation with buoy WEW1 and Schiermonnikoog Noord since the built-in function to do this in Delft3D WAVE (“CondSpecAtDist”) currently does not work for curvilinear grids. Therefore, the measured wave conditions by buoy WEW1 were used for the northern boundary (Figure 38). Wave conditions for the eastern boundary are not specified since the wave direction was in a southeastern direction which means that any waves would immediately leave the model. The wave conditions found for the buoys Amelander Zeegat 2.2 and 5.2 were used for the western boundary.

During the peak of the storm, the  $H_{m0}$  values at the boundaries varied between 1.15 m for the southwestern boundary, 4.58 m for the northwestern boundary and 7.10 m for the northern boundary.

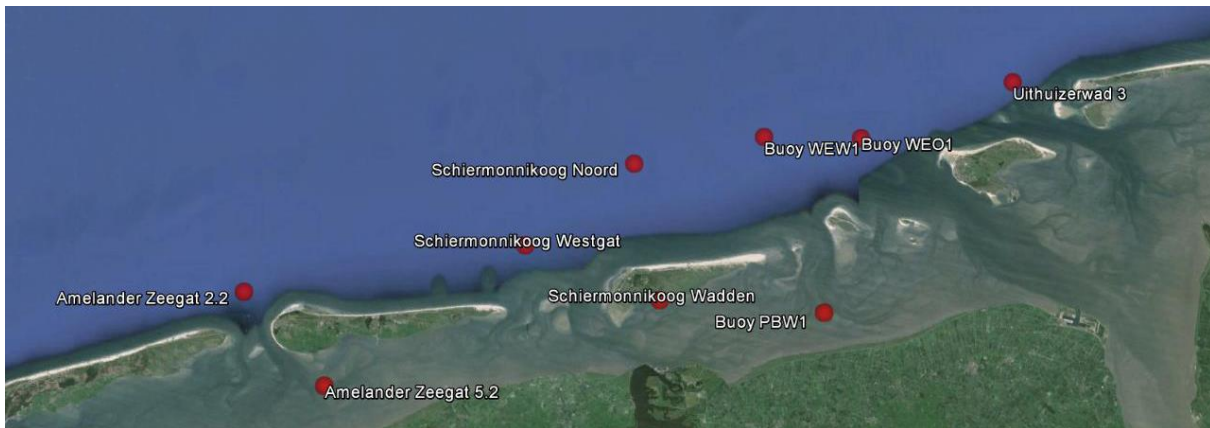


Figure 41 Available wave measurement locations

### FLOW settings

The physical parameter settings in Delft3D determine how the FLOW module responds to the input from the boundary conditions and wind. The water density for salt water varies depending on the temperature of the water and the salinity. Since measurements are not available, it is assumed to be 1025 kg per m<sup>3</sup> which is a generally accepted estimate for salt water (Holthuijsen, 2007).

The Manning bed roughness  $K_N$  value was set at a uniform value 0.004, determined by manual calibration. This was done since there is not enough information available to let the bed roughness vary spatially. That would require information regarding grain size and bed forms. Although the grain size is known for several locations in the eastern Wadden Sea, information regarding the bed forms is unknown. Creating a spatially varying bed roughness based only on grain size would add a false sense of accuracy (Adema, Geleynse, & Telenta, 2014; Ridderinkhof, 1990). The horizontal eddy viscosity was set to 5.

<i>Gravitational acceleration</i>	9.81	[m s <sup>-2</sup> ]
<i>Water density</i>	1025	[kg m <sup>-3</sup> ]
<i>Manning bed roughness</i>	0.004	[s m <sup>-1/3</sup> ]
<i>Horizontal eddy viscosity</i>	5	[m <sup>2</sup> s <sup>-1</sup> ]

The air density  $\rho_a$ , wind velocity at 10 meters height  $U_{10}$  and the wind drag coefficient  $C_d$  are needed to determine the wind shear stress  $\tau_s$  (Eq. 9). A higher drag coefficient means that the water surface is considered more rough due to waves and imperfections forming as a result of the wind. Higher wind speeds cause the roughness of the water surface to increase, which in turn allows for an increased transfer of energy from wind to water, influencing the currents. For the wave calculations, a different approach is used to determine the wind-wave interaction.

$$\tau_s = \rho_a C_d U_{10}^2$$

Eq. 9

The wind drag coefficients for wind velocities 0 and 100 m/s are 0,00063 and 0,00723, respectively, which are the standard values in Delft3D. Even though research has shown that the value for the drag coefficient does not increase linearly for increasing wind velocities, it is an accurate approximation (Hwang, 2005).

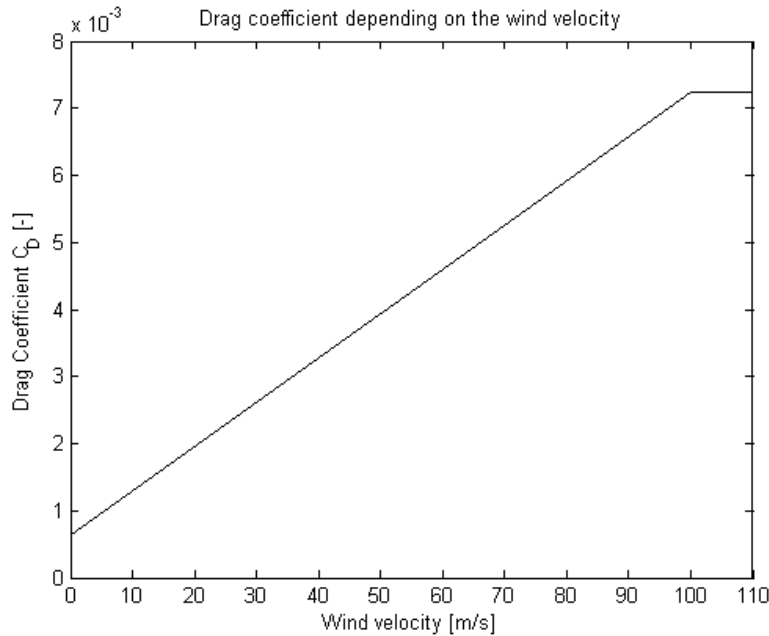


Figure 42 Drag coefficient for wind-water interaction

### WAVE settings

The WAVE module calculates in stationary mode. This was necessary to lower the computing time, which was several days in non-stationary. An alternative is to run non-stationary calculations with hotstart files to continue the calculations from a certain point in time. This however does mean that calibration of the model would have taken significantly longer.

The breaker parameter  $\gamma$  is 0.79, equal to 1D. The quadruplet and trilinear interactions were enabled. The Lumped Trilinear Approximation method was used for the trilinear interactions (Eldeberky & Battjes, 1996), with standard values for triad parameters:  $\alpha = 0.1$  and  $\beta = 2.2$ . The LTA method has the drawback that the wave period is underestimated in shallow waters (Smith, 2004). Not accounting for trilinear interactions would overestimate the wave period.

The bed roughness was determined using the approach developed by Madsen, discussed in the Chapter 4.1. However, to get the wave dimensions correct as they traveled through the model, the bottom roughness length  $K_N$  was set to 0.4 cm for non-vegetated areas and 3.8 to 6.5 cm for the salt marshes. The different  $K_N$  values represent the variation in vegetation

density which was witnessed and can also be seen using satellite images. These values were found by manual calibration.

## 2D results

This paragraph presents the results of the 2D model for both the FLOW and WAVE modules.

The FLOW module calculated the water levels and flow velocities with an interval of 4 minutes. Figure 43 is an example of the water level for one of the time steps. The water level in this figure varies between 2.2 and 3.2 m +NAP. At the location of the pressure sensors, the water level has a maximum of 3.03 m +NAP.

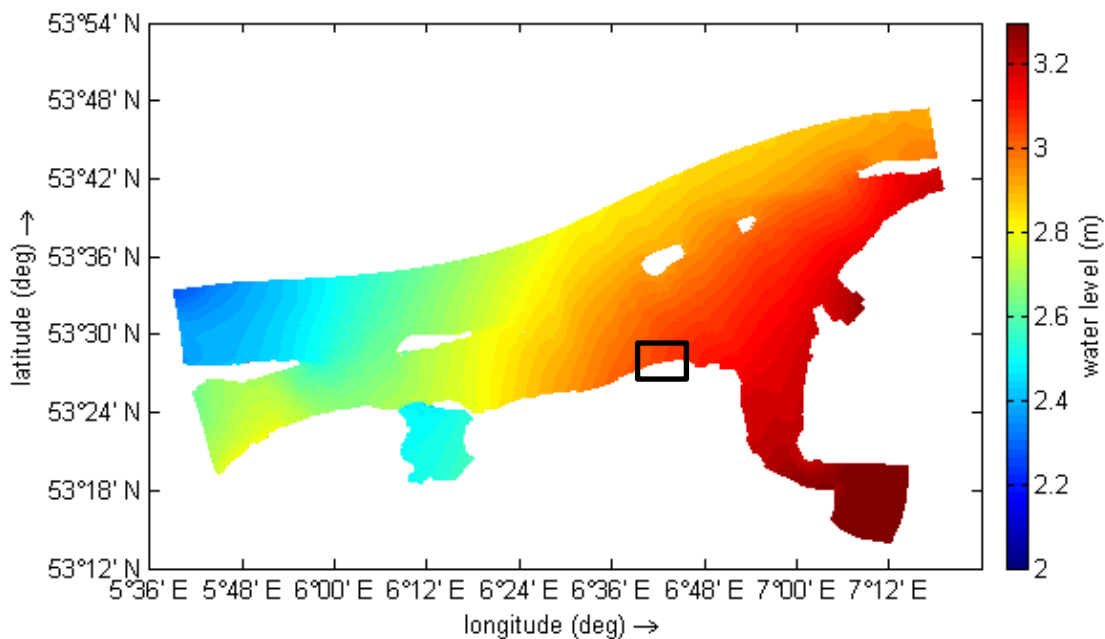


**Figure 43** The calculated water level at January 11<sup>th</sup> 00:30, the location of the pressure sensors is shown by the black rectangle

The maximum difference in water level between the model and the measurements is 5 cm. Figure 44 shows the calculated and measured water levels for pressure sensor 1. The main error is the timing of the model compared to the measurements, lagging by approximately 30 minutes. For a location near the northern border of the model at the Wierumergronden (Figure 45) the water level was measured by Rijkswaterstaat. Comparing the calculations for this location to the measurements, taking into account the timing error, the error is ~5 cm for the peak of the storm. This accuracy is similar to a research performed in the same area (Adema et al., 2014).

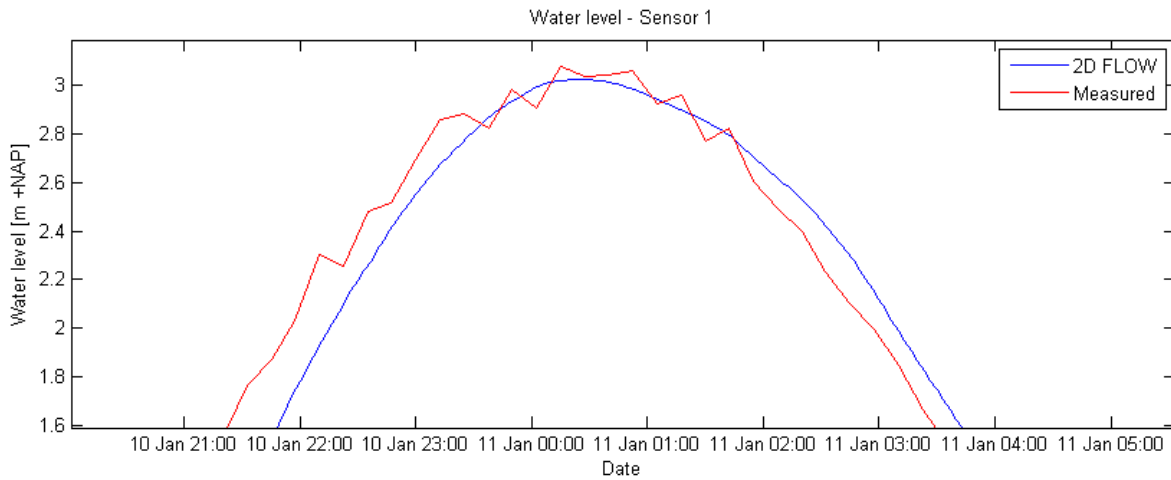


**Figure 44 Measured water level at sensor 1 (red) and the output of the 2D FLOW calculations (blue)**

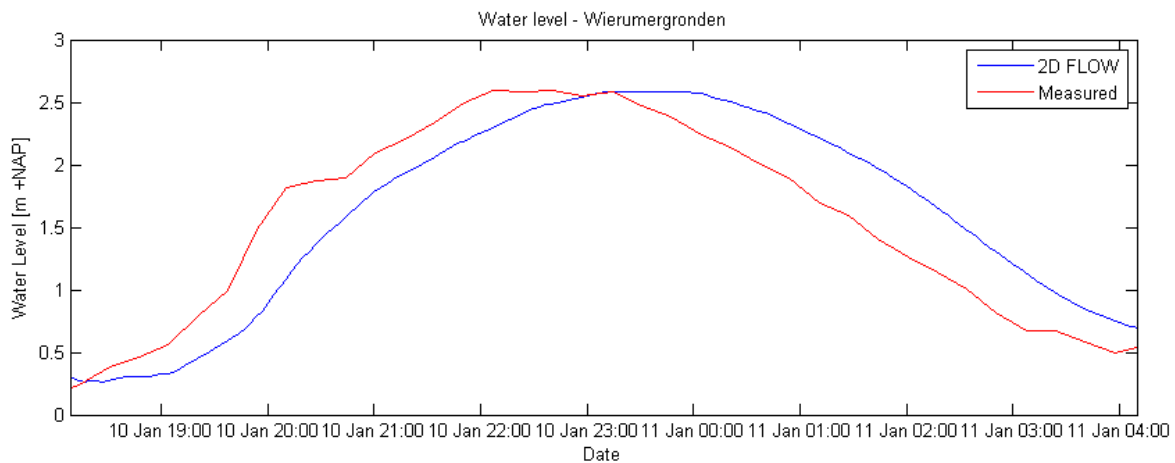


**Figure 45 Measured water level at Wierumergronden (red) and the output of the 2D FLOW calculations (blue)**

The WAVE module calculated the wave characteristics. The  $H_{m0}$  (Figure 46) is approximately 6 m at the northern boundary and then largely dissipates due to the reduced water depth and obstruction by the barrier islands. As a result of the different source terms which dissipate or add energy from the waves (bottom friction, depth-induced wave-breaking and wave growth by wind), the  $H_{m0}$  at the edge of the salt marsh is 0.74 m (Figure 48, Figure 49).

The wave direction which was unknown for the 1D model, is now calculated (Figure 47). This suggests that the difference between the direction of the 1D model and the waves is approximately  $30^\circ$ . If these wave directions are correct, the calibrated 1D model is compensating for dissipation that in reality took place over a distance of 115%.

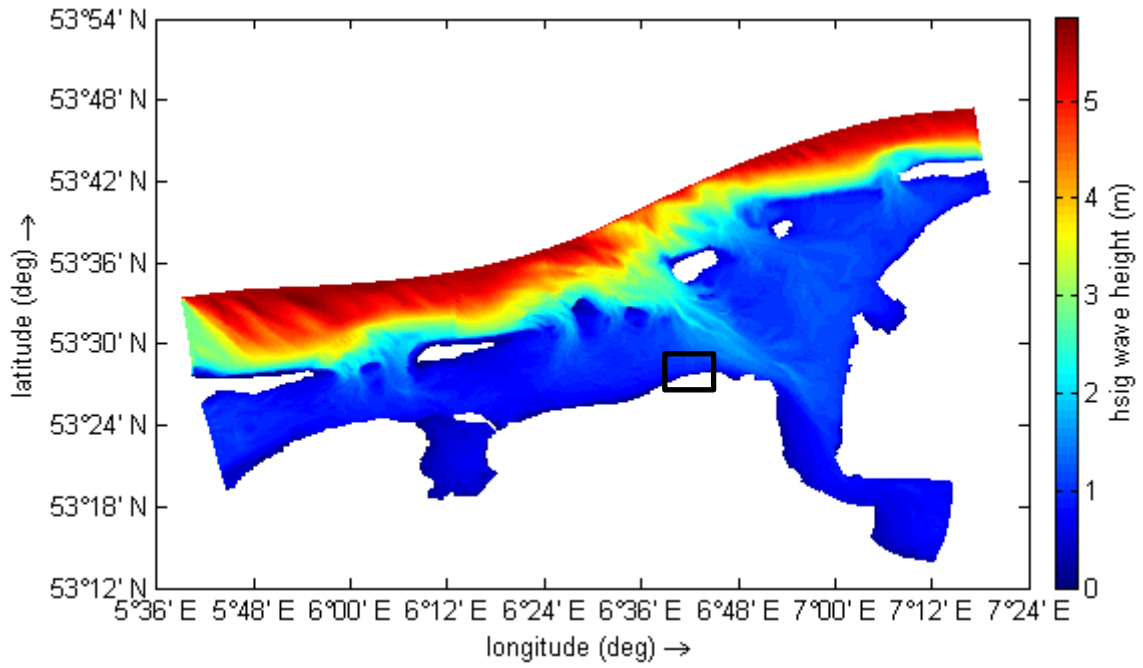


Figure 46 The calculated  $H_{m0}$ , the location of the pressure sensors is shown by the black rectangle

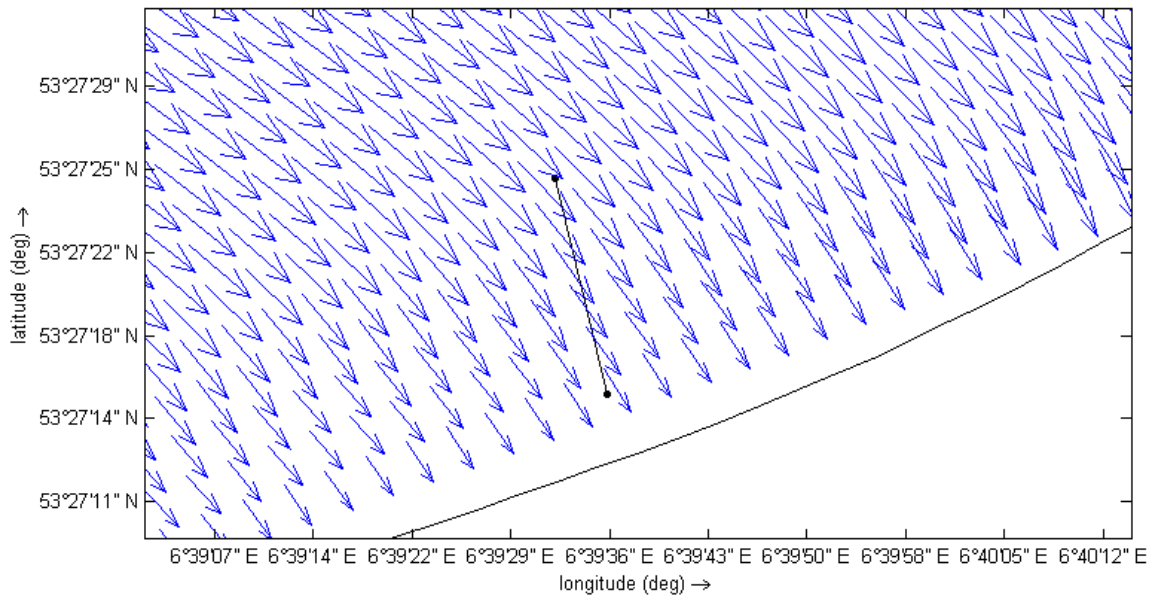


Figure 47 The calculated mean wave direction at the test site, showing the location of the 1D model

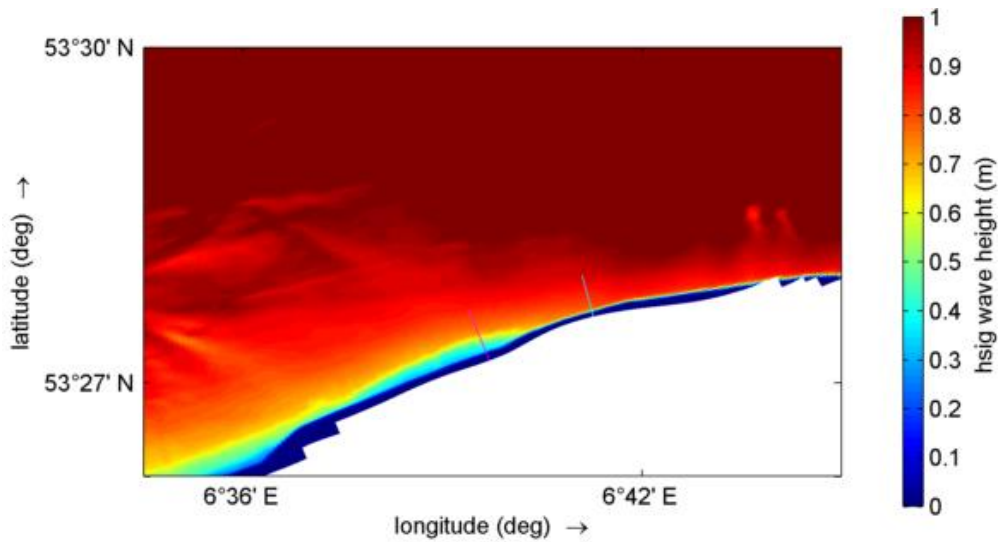


Figure 48  $H_{m0}$  near the dike at the location of the pressure sensors (see Figure 46), the colored cross-sections are found in the next figure

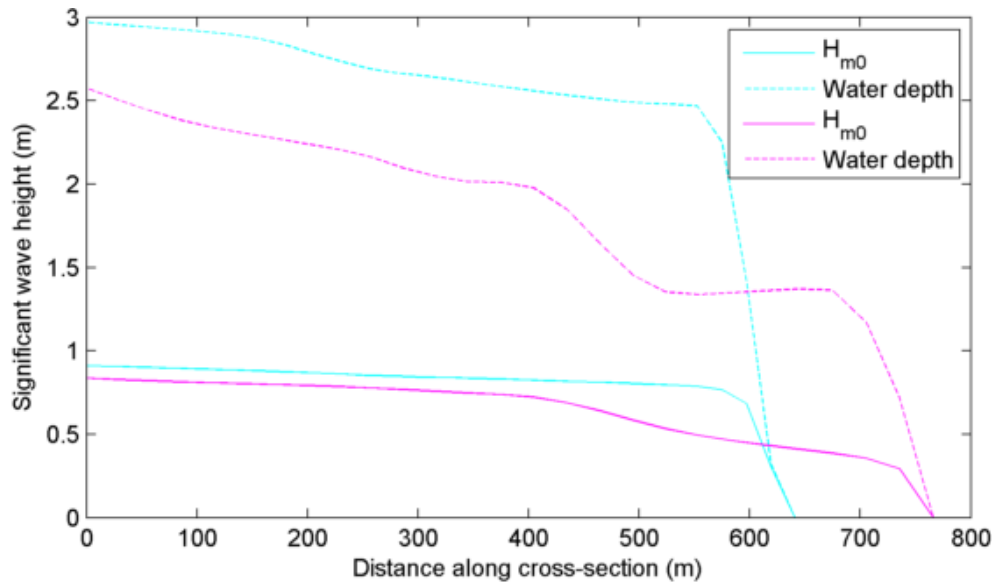


Figure 49 Water depth and  $H_{m0}$  results for cross-sections shown in the previous figure

The results in Figure 48 and Figure 49 show that the foreshore conditions have a notable influence on the wave conditions near the dike. The lower bed level east of the vegetated area limits the water depth to 2.5 – 3.0 meters depth during the storm, where the incoming waves are not dissipated further. Depth-induced wave-breaking is limited since  $H_{m0}/d$  does not approach the breaker parameter  $\gamma = 0.79$ . Comparing  $H_{m0}$  between areas with a vegetated foreshore and areas without, there is a clear difference. The waves are significantly reduced at locations where the bed level is higher and water depths reduced. (Figure 48, Figure 49). The  $H_{m0}$ , wave period  $T_{m-1,0}$  and peak wave period  $T_p$  are compared for several locations (Table 3). This table shows that the average error for  $H_{m0}$  over four locations is 2 cm.  $T_{m-1,0}$  differs largely compared to the measurements, especially for the

shallow areas where the sensors are located. The water depth near the sensors was <3 m and >8.5 m for the location of the buoy. The value for  $T_p$  is more accurately reproduced.

The better performance of the model in reproducing the peak period can be explained by the fact that the equations used to determine  $T_{m-1,0}$  (Eq. 10, Eq. 11) give a high weight to low frequencies in the wave spectrum due to the negative power for  $m_{-1}$ . Any differences between the model outcomes and the measurements in the low end of the wave spectra have a large influence for the value for  $T_{m-1,0}$ . The value for  $T_p$  is determined by the peak in the wave spectrum which is less influenced by small changes.

$$T_{m-1,0} = m_{-1}/m_0 \tag{Eq. 10}$$

$$m_n = \int_{f_1}^{f_2} E(f) * f^n df \tag{Eq. 11}$$

**Table 3 Comparison of the values for  $H_{m0}$  and the corresponding wave periods  $T_{m-1,0}$  and  $T_p$  for three of the sensors and the buoy named Schiermonnikoog Westgat located in deep water**

		Sensor 1	Sensor 5	Sensor 8	Buoy Sch. Westgat
$H_{m0}$ [m]	<i>Measured</i>	0.77	0.36	0.74	4.61
	<i>Model outcome</i>	0.74	0.38	0.71	4.60
$T_{m-1,0}$ [s]	<i>Measured</i>	5.7 - 7.5	9.5 - 10.5	7.5 - 12	10.8 - 11.1
	<i>Model outcome</i>	2.9	2.2	3.2	9.0
$T_p$ [s]	<i>Measured</i>	3.5 - 5.0	1.5 - 1.8	3.7 - 3.8	12.5 - 14.3
	<i>Model outcome</i>	3.5	3.5	3.8	10.7

The possible cause for the underestimation of  $T_{m-1,0}$  is shown in Figure 50 which illustrates how the wave spectrum is influenced by the different processes. The triad wave-wave interactions redistribute the energy from the peak of the spectrum to higher and lower frequencies. However, in the SWAN model the energy is only shifted from the peak to higher frequencies (Buckley & Lowe, 2013). This results in an underestimation of the energy in the lowest frequencies (large wave periods) which leads to underestimation of the value for  $T_{m-1,0}$  (Figure 51) while it can be seen that the value for  $T_p$  calculated with the model is close to the measured values for  $T_p$ .

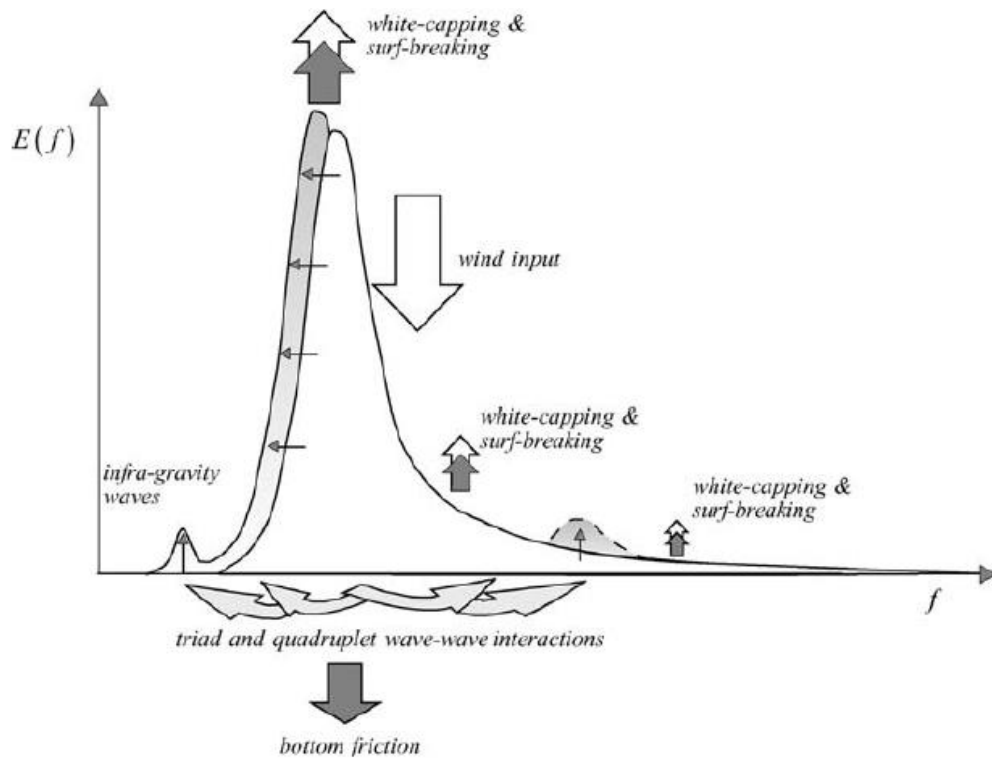


**Figure 50** The influences on the wave spectrum by the different processes (Holthuijsen, 2007)

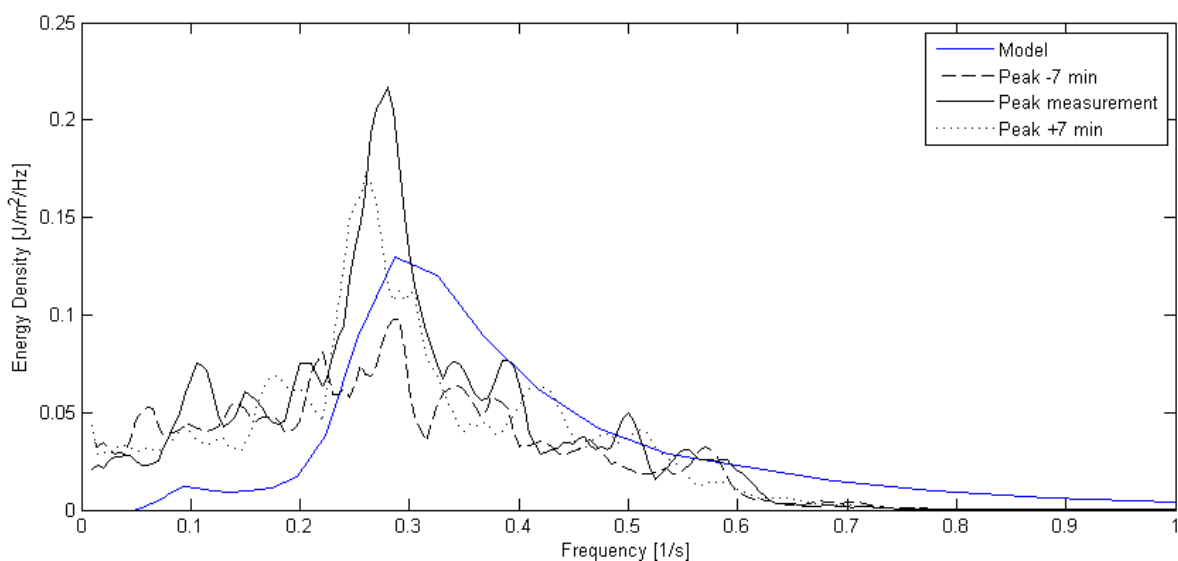


**Figure 51** Measured wave spectra for sensor 1 (edge of the salt marsh) around the peak of the storm with the calculated wave spectrum for this location

## 5. Flotsam level reproduction

The 2D model outcomes are now used to replicate the measured flotsam levels which were the result of the storm on January 11<sup>th</sup> 2015. This is done using the method to determine the maximum wave run-up described in Chapter 2.2 (EurOtop, 2007). First the 2% wave run-up height  $R_{u2\%}$  is determined using Eq. 12.

$$R_{u2\%} = 1.65H_{m0} * \tan \alpha / \sqrt{H_{m0} / \left( \frac{9.81T_{m-1,0}^2}{2\pi} \right)} * (1 - 0.0063|\beta|) \quad \text{Eq. 12}$$

The 2D model is used to determine the following variables (Table 4): water level  $\xi$  [m +NAP], significant wave height  $H_{m0}$  [m], mean wave period  $T_{m-1,0}$  [s] and wave angle [°].

The direction of the normal of the dike sections, and slope  $\alpha$  [°] were determined using accurate GPS measurements performed by the water board Noorderzijlvest. The angle of wave attack  $\beta$  [°] is found by comparing the local wave angle to the normal of the local dike section.

**Table 4 Variables used for flotsam level calculations**

<i>Variable</i>	<i>Minimum</i>	<i>Maximum</i>	<i>Average</i>
$H_{m0}$	0.37	0.74	0.51
$T_{m-1,0}$	2.08	2.95	2.50
$\xi$	2.98	3.04	3.01
$\alpha$	11	17	15.7
$\beta$	18	40	30.0

As explained in Chapter 2.2, the factor  $\gamma_{max}$  which is multiplied with  $R_{u2\%}$  to calculate  $R_{umax}$  (Eq. 13) varies between 1.17 and 1.40 (de Reus, 1983).

$$R_{umax} \approx \gamma_{max} * R_{u2\%} \quad \text{Eq. 13}$$

When the calculated maximum wave run-up for  $\gamma_{max} = 1.17$  and  $\gamma_{max} = 1.40$  is compared to the measurements for the flotsam levels (Figure 52, Figure 53), it is seen that the pattern displayed by the measurements is reproduced. The estimated accuracy of the flotsam measurements ( $\pm 0.4$  m) is illustrated by the dashed lines.

Salt marshes were present for all locations up to the 21 km mark. For the locations without the salt marshes, the calculations underestimate the measurements or are just inside the

estimated accuracy of the measured flotsam level. This can have several causes. The first and most likely cause is that the wave period  $T_{m-1,0}$  is underestimated with the 2D model by a factor 2 or more compared to the pressure gauge measurements. The reason for this was explained in Chapter 4.2. The second cause are errors in the other parameters. Although it was seen that the  $H_{m0}$  is accurate for locations where we have measurements, errors are still possible. For example, the wave direction is calculated with the 2D model and since there are no near-shore measurements of the wave direction, it is not possible to judge the quality of these values. However, the directions are realistic when inspected visually (Figure 47) since the waves travel in a southwestern direction and refract towards the dike.

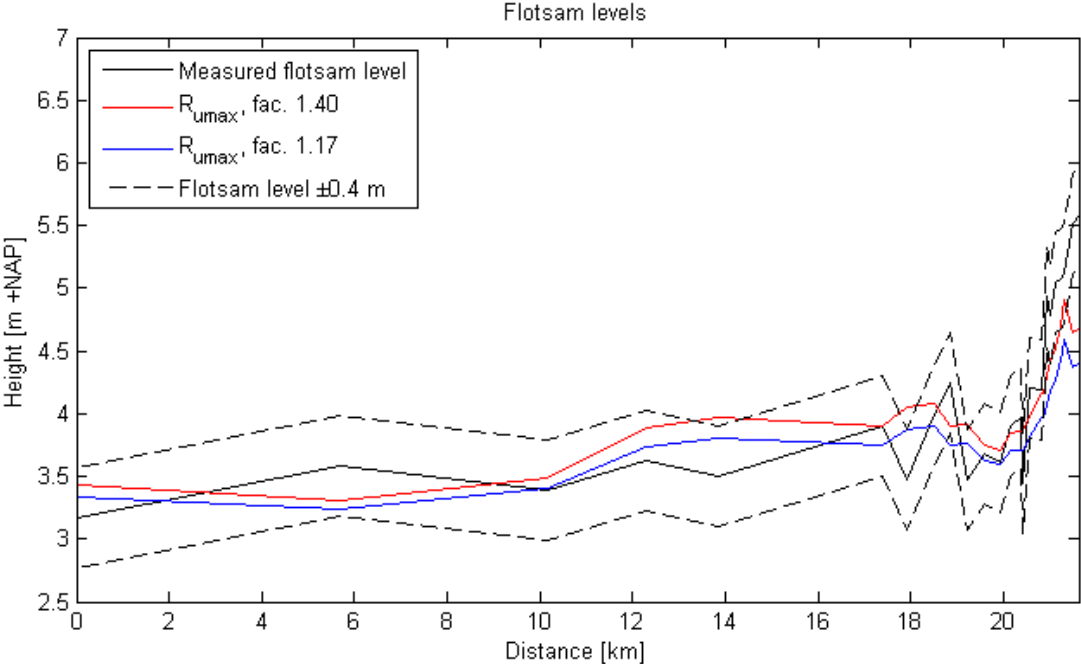


**Figure 52** The measured flotsam levels and calculated maximum wave run-up. The dashed lines show the estimated accuracy of the flotsam measurements

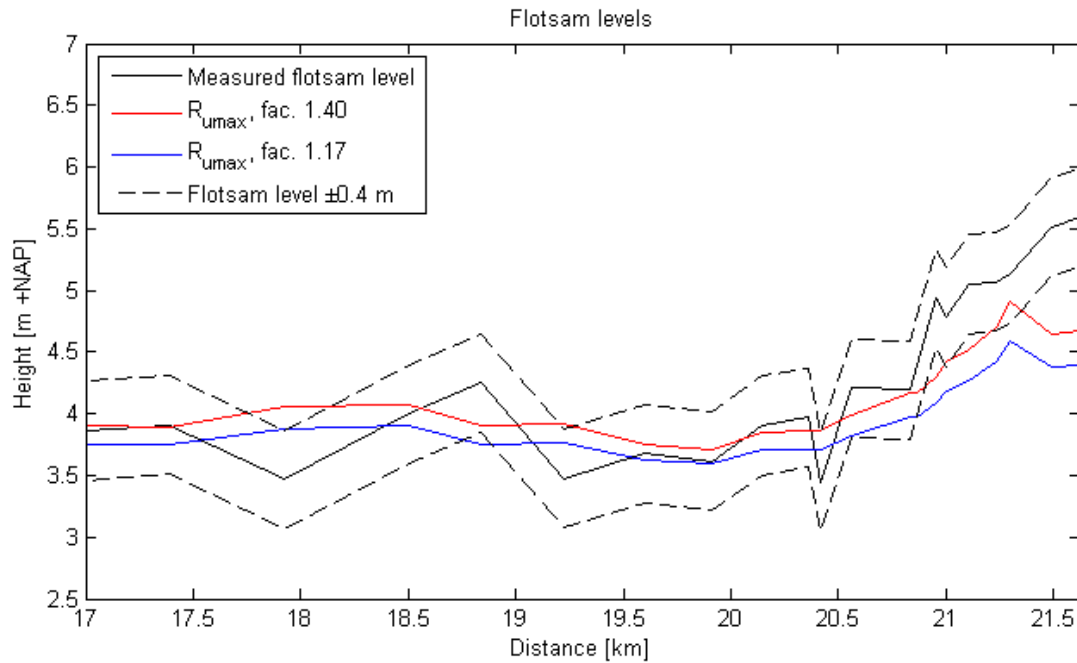


Figure 53 The eastern measured flotsam levels and calculated maximum wave run-up

By multiplying the values for  $T_{m-1,0}$  by a factor 2, the calculated maximum wave run-up increases (Figure 54, Figure 55). The higher flotsam levels are now more properly replicated at the cost of accuracy for the lower flotsam levels. This suggests that either the wave period  $T_{m-1,0}$  is not significantly underestimated for all locations, or that one or more of the other parameters ( $H_{m0}$ ,  $\alpha$ ,  $\beta$ ,  $\xi$ ) are overestimated for these locations.

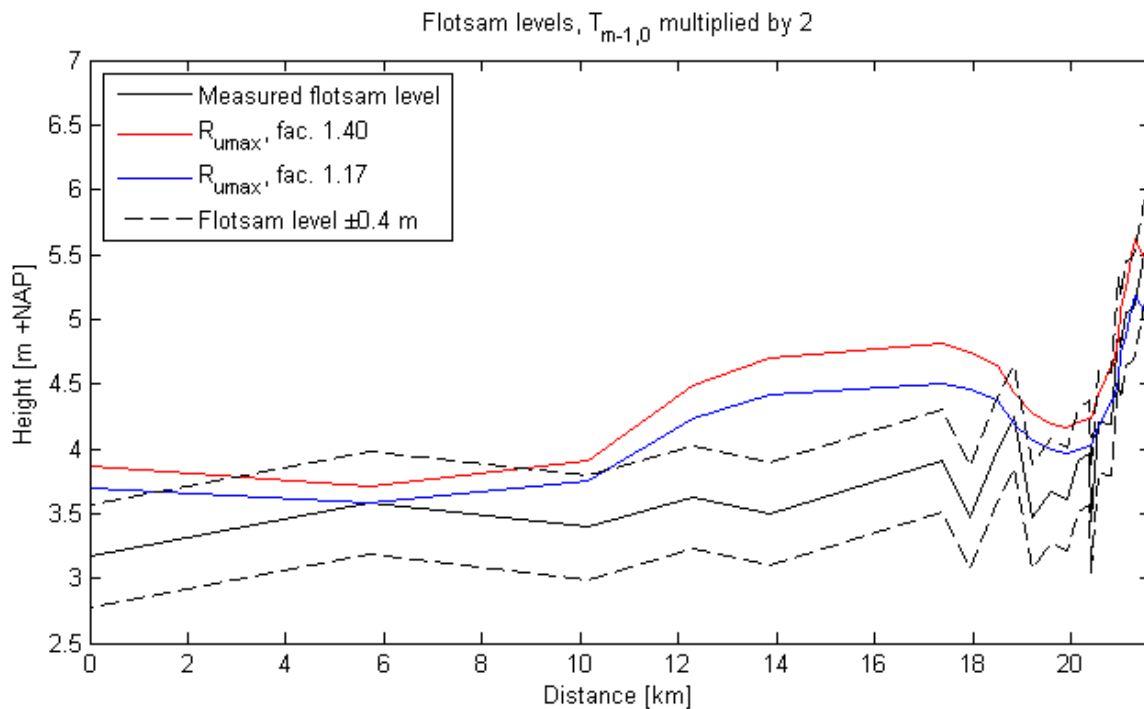


Figure 54 The measured flotsam levels and calculated maximum wave run-up for  $T_{m-1,0} * 2$

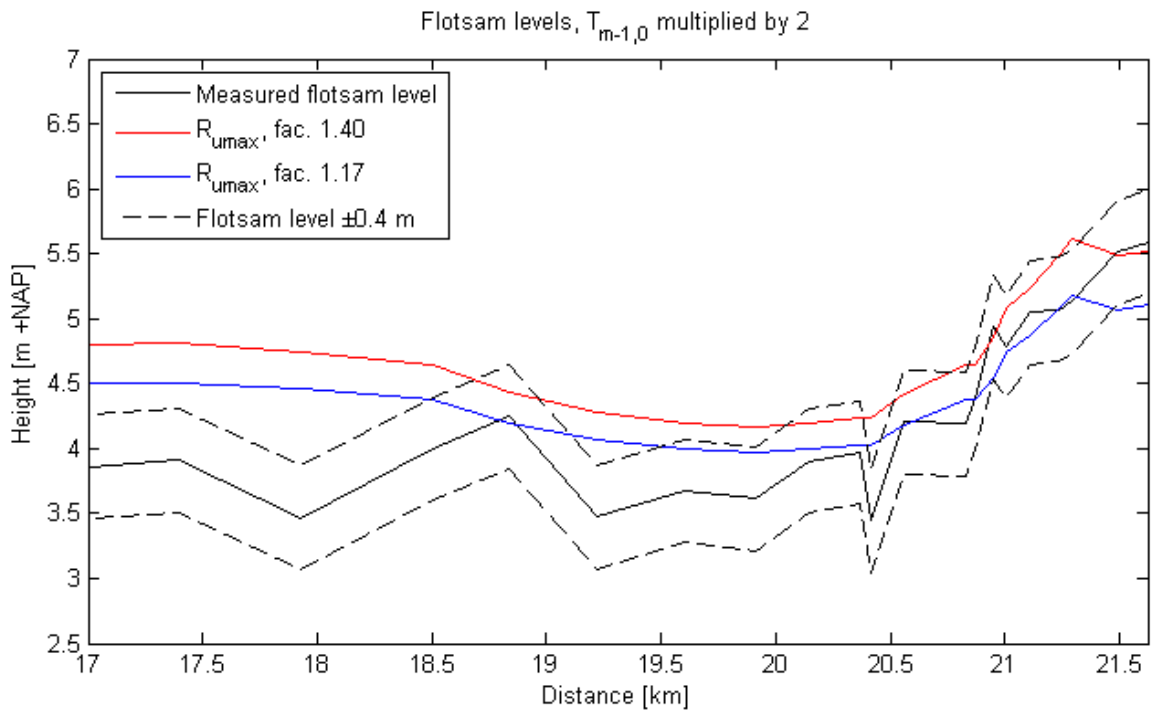


Figure 55 The eastern measured flotsam levels and calculated maximum wave run-up for  $T_{m-1,0} * 2$

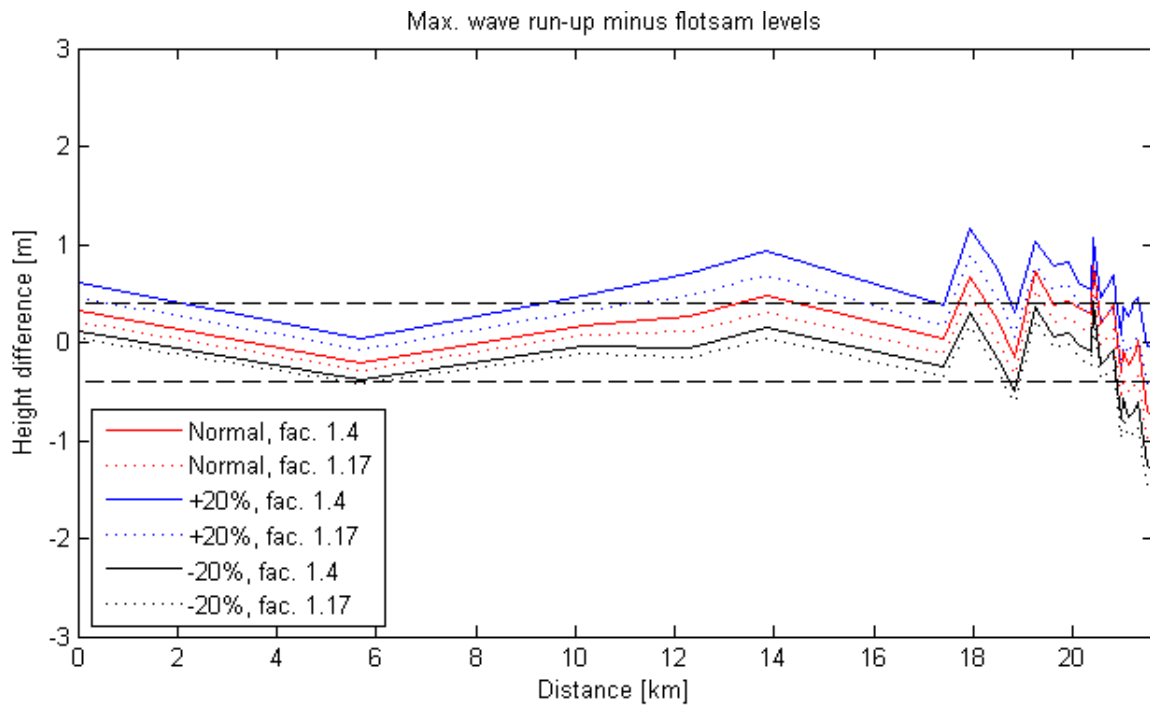
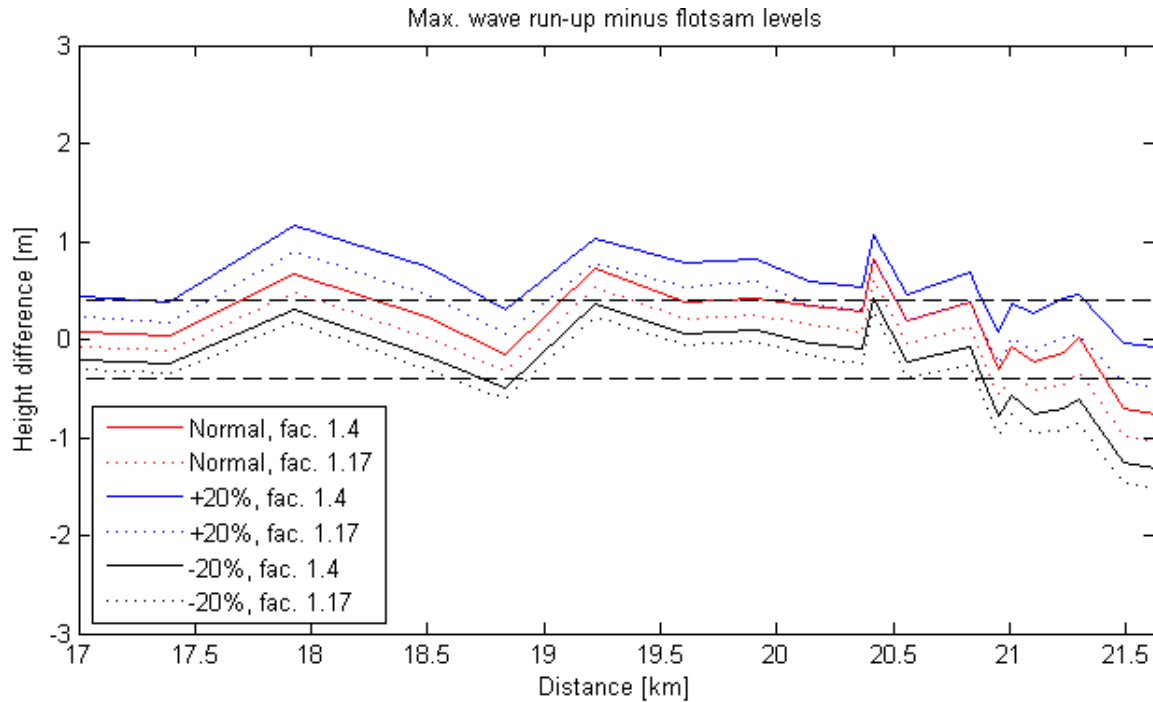


Figure 56 The calculated maximum wave run-up minus the measured flotsam levels. The parameters used in the run-up calculation (red) are changed by 20% to result in a low (black) or high (blue) estimate.



**Figure 57** The calculated maximum wave run-up minus the measured flotsam levels for the eastern locations. The parameters used in the run-up calculation (red) are changed by 20% to result in a low (black) or high (blue) estimate.

### Summary

The goal of the calculations performed in this chapter was to see how accurately the measured flotsam levels can be reproduced using the results from a 2D model. The results show that it is possible to reproduce the pattern found in the measurements and reproduce the measurements to within the estimated accuracy of the measurements for most locations. However, since the accuracy of the measurements is  $\pm 0.4$  m due to the variable nature of the flotsam, it is not an exact approach to e.g. validate the wave conditions calculated in a 2D SWAN model.

## 6. Scenario analysis

Scenarios are created to simulate the effect of severe changes to the salt marshes. By applying the 1/4000 years design conditions at the test site, it is possible to find the influence of different foreshore conditions. The same changes are tested in the 1D and 2D models where possible.

For the location near the eastern edge of the salt marsh, the dike section is known as “Waddenzee 0779”. For this location, the design conditions are: a water level of 5.3 m +NAP and a value for  $H_{m0}$  of 2.0 m with  $T_{m-1,0} = 4.95$  s. This can be found in the WTI2011 (Wettelijk Toetsinstrumentarium 2011). These values are determined for dike sections with lengths of several kilometers which means that calculations are based on the highest waves in the area, not taking the salt marshes into account since these are not present on all locations. The wind is coming from the northwest (300°) with a velocity of 35.7 m/s. By applying these conditions at the edge of the salt marsh in the 1D model, the effect of the salt marsh during the design conditions can be seen. For the 2D model, the water level and wind conditions resulted in waves of ~2.0 m for locations without vegetation east of the salt marsh.

### 6.1. Scenarios

For the 1D and 2D model, similar scenarios are developed (Table 5). Design conditions are applied to all scenarios.

Table 5 The different scenarios per model

1D hydraulic boundary scenarios	2D hydraulic boundary scenarios
Vegetation as bed roughness	Current situation
Vegetation as vertical cylinders	Longer salt marsh
No vegetation	No vegetation
Lower bed salt marsh, no vegetation	Lower bed salt marsh, no vegetation
Increased bed level salt marsh	Increased bed level salt marsh

#### *Vegetation as bed roughness*

The calibrated models discussed in Chapter 4 are applied. The vegetation is schematized as bed roughness in both models. Bottom roughness length in the 1D model  $K_N = 0.1$  m. In the 2D model  $K_N = 0.065$

#### *Vegetation as vertical cylinders (1D only)*

The vegetation in 1D is schematized as vertical cylinders with vegetation drag parameter  $C_D = 0.65$ . This approach was discussed in Chapter 4. This schematization of the vegetation is not possible in the 2D model.

*Longer salt marsh (2D only)*

For this scenario, the foreshore is extended by approximately 1200 meters. This scenario shows the of a much longer salt-marsh. To do this, the bed level of the extension is modified to a minimum of 1.00 m +NAP and the additional bed roughness as a result of the vegetation is applied.

*No vegetation*

The vegetation is removed from the models. For the 1D model the vegetation drag parameter  $C_D = 0$  and bottom roughness length  $K_N = 0.001$  m. For the 2D model  $K_N = 0.004$  m at all locations.

*Lower bed salt marsh, no vegetation*

The vegetation is removed, similar to scenario 3. In addition to this, the bed level is lowered to match locations where the salt marshes are not present. This means that the bed level is lowered by between 0.9 and 1.2 m to a maximum of 0.3 m +NAP.

*Increased bed level salt marsh*

The bed level on the salt marsh is increased by 1.0 m. This simulates the effect of a large sand-nourishment in the area. In the 1D model, the vegetation is simulated as vertical cylinders.

## 6.2. 1D scenario results

The results of the 1D scenarios are given in this chapter. Table 6 presents the wave characteristics for the different scenarios and

Table 7 presents the changes between the edge of the salt marsh and the toe of the dike.

The two approaches for vegetation schematization result in different outcomes (Table 6, Figure 58). Vegetation as additional bed roughness results in a higher value for  $H_{m0}$  compared to schematization as vertical cylinders, 1.33 and 1.28 m respectively. The mean wave period  $T_{m-1,0}$  here is lower, which is in line with previous research (Hu et al., 2012). The method used to take vegetation into account is therefore relevant to the calculated wave heights.

Removing vegetation leads to a significant wave height,  $H_{m0}$  of 1.62 m and for locations where higher bed level and dissipation by vegetation are absent, the wave height is 1.98 m. This is fully in line with the design conditions for the dike section. Increasing the bed level by 1 meter reduces the  $H_{m0}$  further to 1.02 m, a reduction of 49%. The energy of the waves  $E$  (Eq. 14), is then reduced by 74%, compared to 56-59% under current conditions.

The dominant dissipative term differs for the different scenarios. Changes in bed level significantly increases depth-induced wave-breaking. Wave-breaking mainly occurs at the edge of the marsh while dissipation by vegetation continues over the length of the marsh. (Appendix A).

$$E = \frac{1}{8} \rho g H_{rms}^2 \quad \text{Eq. 14}$$

**Table 6 The wave characteristics for the different 1D scenarios and the edge of the salt marsh**

	$H_{m0}$ [m]	$T_p$ [s]	$T_{m-1,0}$ [s]	$E$ [J/m <sup>2</sup> ]
Edge of the salt marsh	2.00	4.94	4.47	2514
<i>Vegetation as bed roughness</i>	1.33	4.94	4.06	1112
<i>Vegetation as vertical cylinders</i>	1.28	4.98	4.52	1030
<i>No vegetation</i>	1.62	4.96	4.33	1649
<i>Lower bed salt marsh, no vegetation</i>	1.98	4.96	4.35	2464
<i>Increased bed level salt marsh</i>	1.02	4.97	4.03	654

**Table 7** The change in  $H_{m0}$  and  $E$  as waves travel from the edge of the salt marsh to the toe of the dike for the different scenarios

	$\Delta H_{m0}$ [m]		$\Delta E$ [J/m <sup>2</sup> ]	
<i>Vegetation as bed roughness</i>	-0.67	-34%	-1402	-56%
<i>Vegetation as vertical cylinders</i>	-0.72	-36%	-1484	-59%
<i>No vegetation</i>	-0.38	-19%	-865	-34%
<i>Lower bed salt marsh, no vegetation</i>	-0.02	-1%	-50	-2%
<i>Increased bed level salt marsh</i>	-0.98	-49%	-1860	-74%

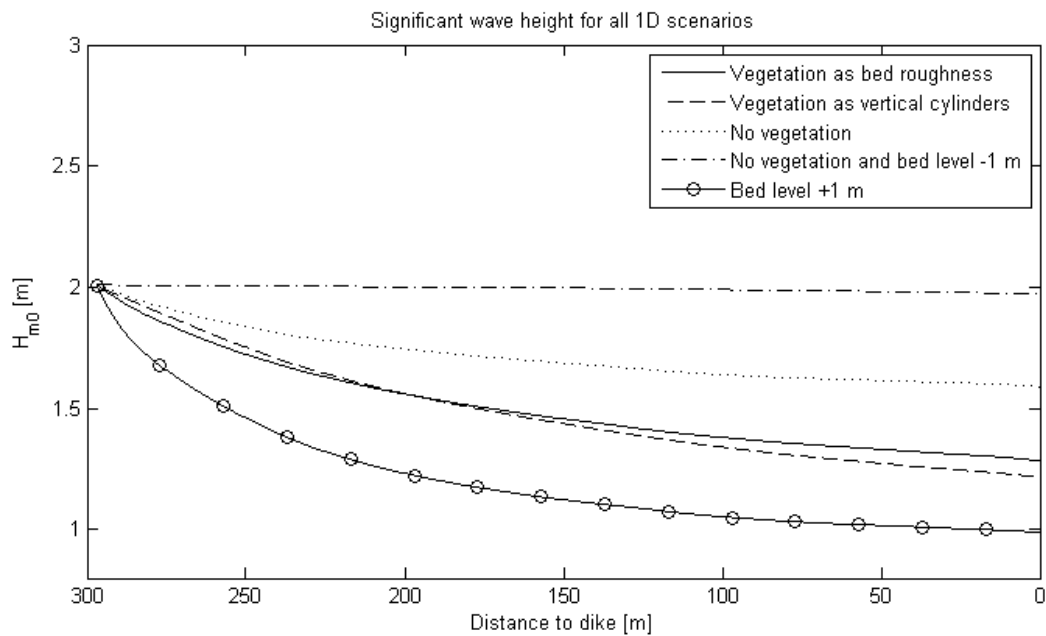


**Figure 58** The significant wave height for the different 1D scenarios, between the edge of the salt marsh (left) and the toe of the dike (right)

### 6.3. 2D scenario results

All the 2D scenario results are presented in this chapter. The calculated significant wave height is shown in Figure 59 with the output location for the other figures and tables illustrated by the black rectangle. The  $H_{m0}$  at the northern border of the model exceeds 7.0 m and is reduced to 1.8 at the edge of the salt marsh. A part of the wave energy is dissipated before the waves reach the vegetated area due to the smaller depth in this area. The wave conditions in Table 8 and Table 9 are determined at the same location as the 1D model results. These results are also shown in Figure 60. The different dissipative terms are shown in Appendix B. These terms show a more fluent transition of the waves than in the 1D model. The dominant dissipation type is dependent on the conditions of the scenario.

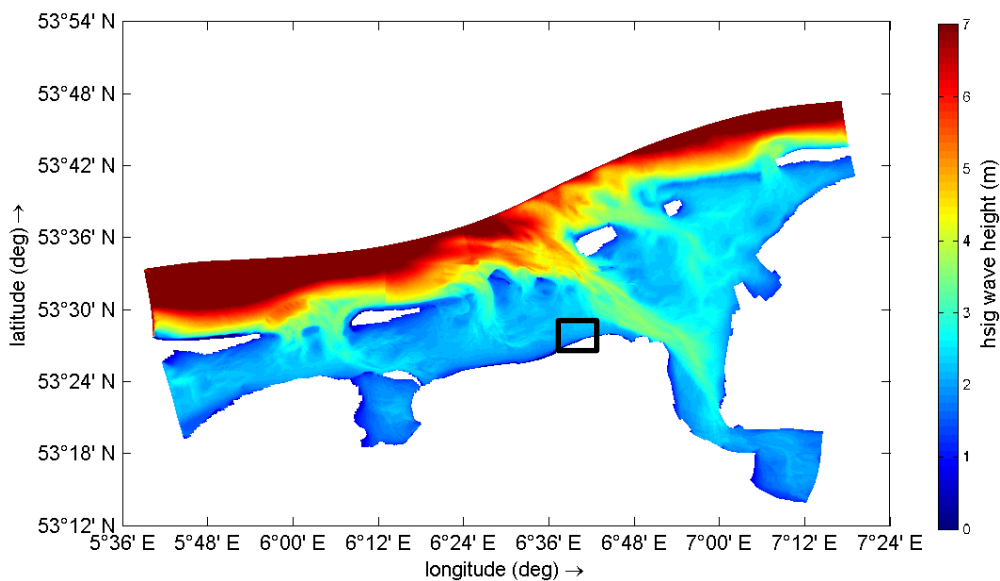


Figure 59 The 2D model under design conditions

Figure 60 shows the effect of the different scenarios for the location of the 1D model. When the 1/4000 event occurs with the salt marsh at its current state,  $H_{m0}$  is reduced to 1.47 m. This is a reduction of 27% compared to the design conditions.

Although it was found in Chapter 4.2 that the 2D model underestimates the lower wave frequencies which are important for the value of  $T_{m-1,0}$ , the results show that without the higher bed level and vegetation present,  $T_{m-1,0}$  increases by 10%. The difference in wave period is seen for all locations on the salt marsh. An absence of the salt marshes therefore results in higher wave run-up and a higher probability of wave-overtopping, caused by higher values for both  $H_{m0}$  and  $T_{m-1,0}$  (EurOtop, 2007).

In the scenario for a longer salt marsh, the bed level is increased to a minimum of 1.0 m +NAP, extending the salt marsh by 1500 m. For this extension, the bed roughness is

increased to simulate the presence of vegetation. Although the length of the salt marsh is now approximately 6 times longer, the additional wave damping is limited.  $H_{m0}$  is reduced by 31% compared to 27% for the current situation. Additionally, the slope seen near the dike in Figure 60 for the current situation is nearly horizontal, which suggests that the different source terms are close to an equilibrium. Such an equilibrium can be seen for the scenario without vegetation and a lower bed level. The difference in bed level can be used to determine the amount of soil needed to implement the salt marsh elsewhere along this coast. This requires approximately 1000 m<sup>3</sup> sand per meter shoreline.

Increasing the bed level by 1.0 m on the salt marsh leads to an additional wave damping of 0.36 m compared to the current situation. It is unlikely that achieving such a bed level rise in the short term is possible in a natural way. However, sea level rise is expected up to 1 cm per year which means that the bed level of the salt marsh can grow on the long term if maintained properly (Dissanayake, Kurunaratna, & Ranasinghe, 2015).

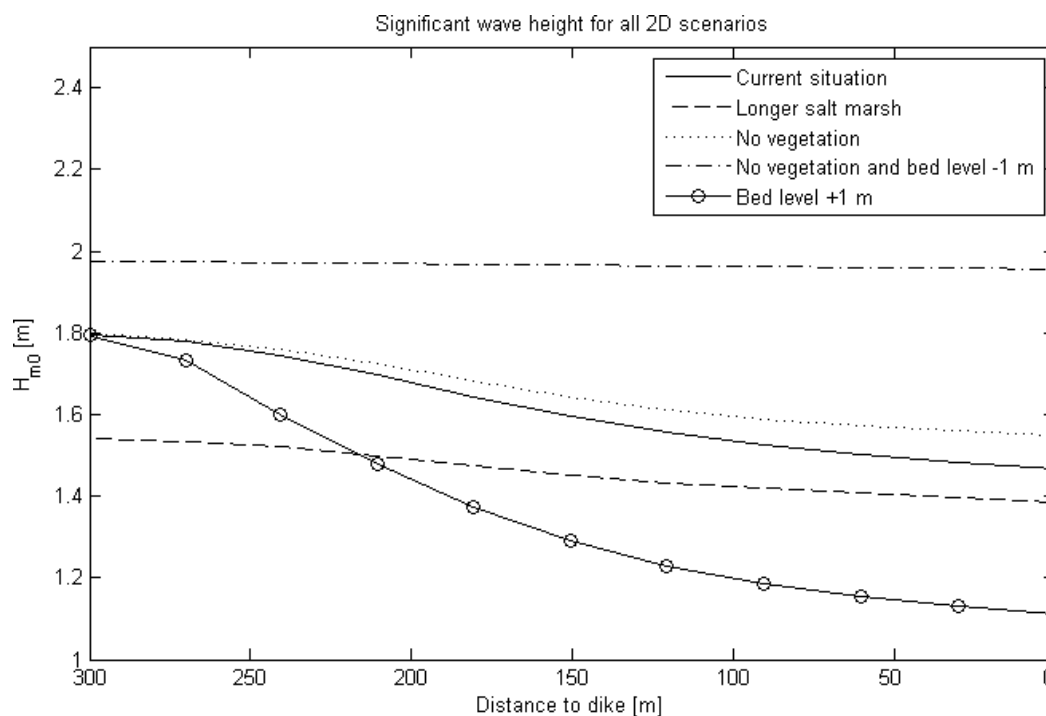


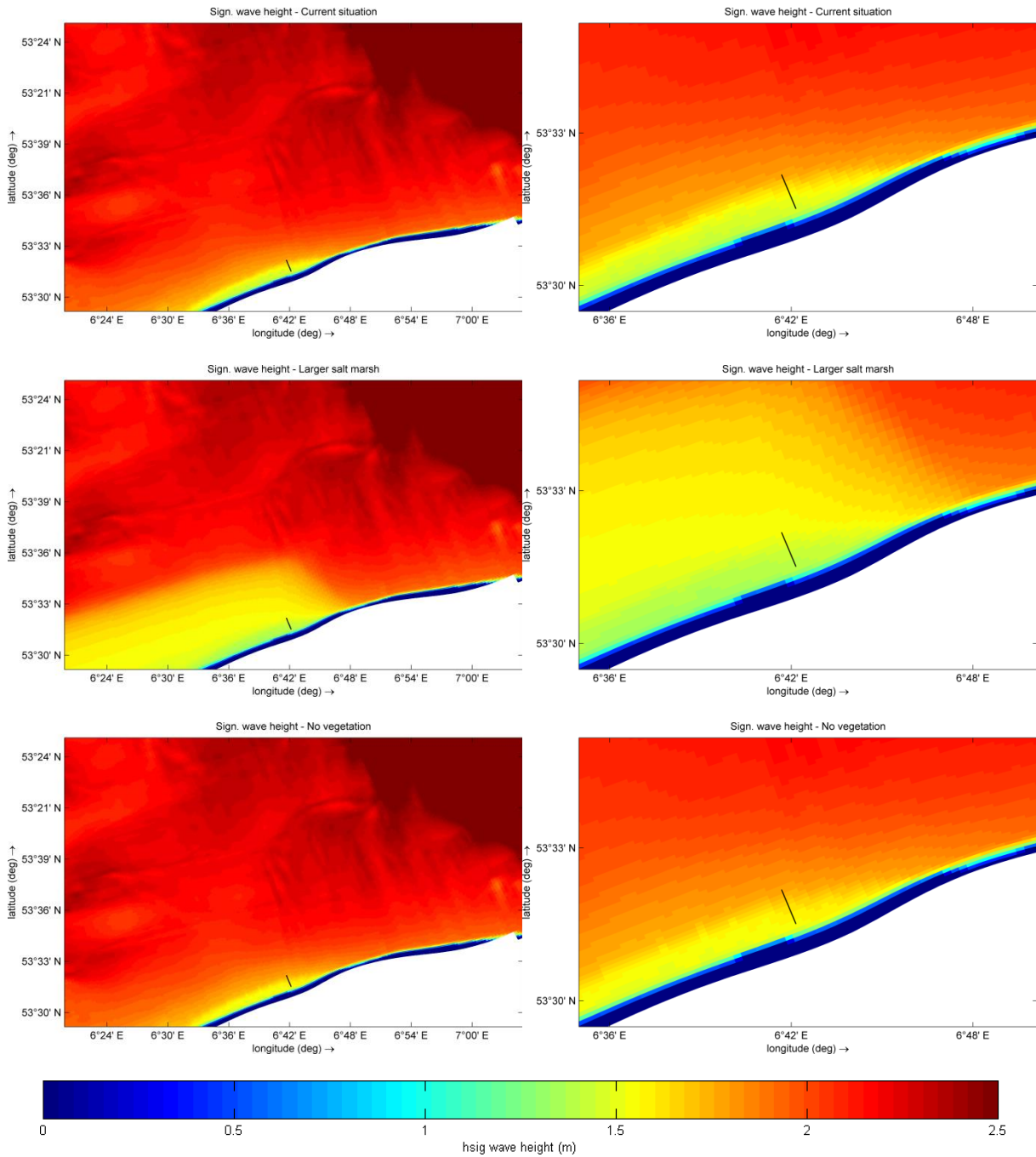
Figure 60 The significant wave height for all 2D scenarios for the location of the 1D model

Table 8 The wave characteristics for the design conditions and the different 2D scenarios at the toe of the dike

	$H_{m0}$ [m]	$T_{m-1,0}$ [s]	$E$ [J/m <sup>2</sup> ]
Design conditions	2.00	4.95	2514
Current situation	1.47	4.07	1358
Longer salt marsh	1.39	3.53	1214
No vegetation	1.55	4.22	1510
Lower bed salt marsh, no vegetation	1.96	4.30	2414
Increased bed level salt marsh	1.11	3.67	774

**Table 9** The change in  $H_{m0}$  and  $E$  as waves travel from the edge of the salt marsh to the toe of the dike for the different scenarios

	$\Delta H_{m0}$ [m]		$\Delta E$ [J/m <sup>2</sup> ]	
<i>Current situation</i>	-0.53	-27%	-1156	-46%
<i>Longer salt marsh</i>	-0.61	-31%	-1300	-52%
<i>No vegetation</i>	-0.45	-23%	-1004	-40%
<i>Lower bed salt marsh, no vegetation</i>	-0.04	-2%	-100	-4%
<i>Increased bed level salt marsh</i>	-0.89	-45%	-1740	-69%



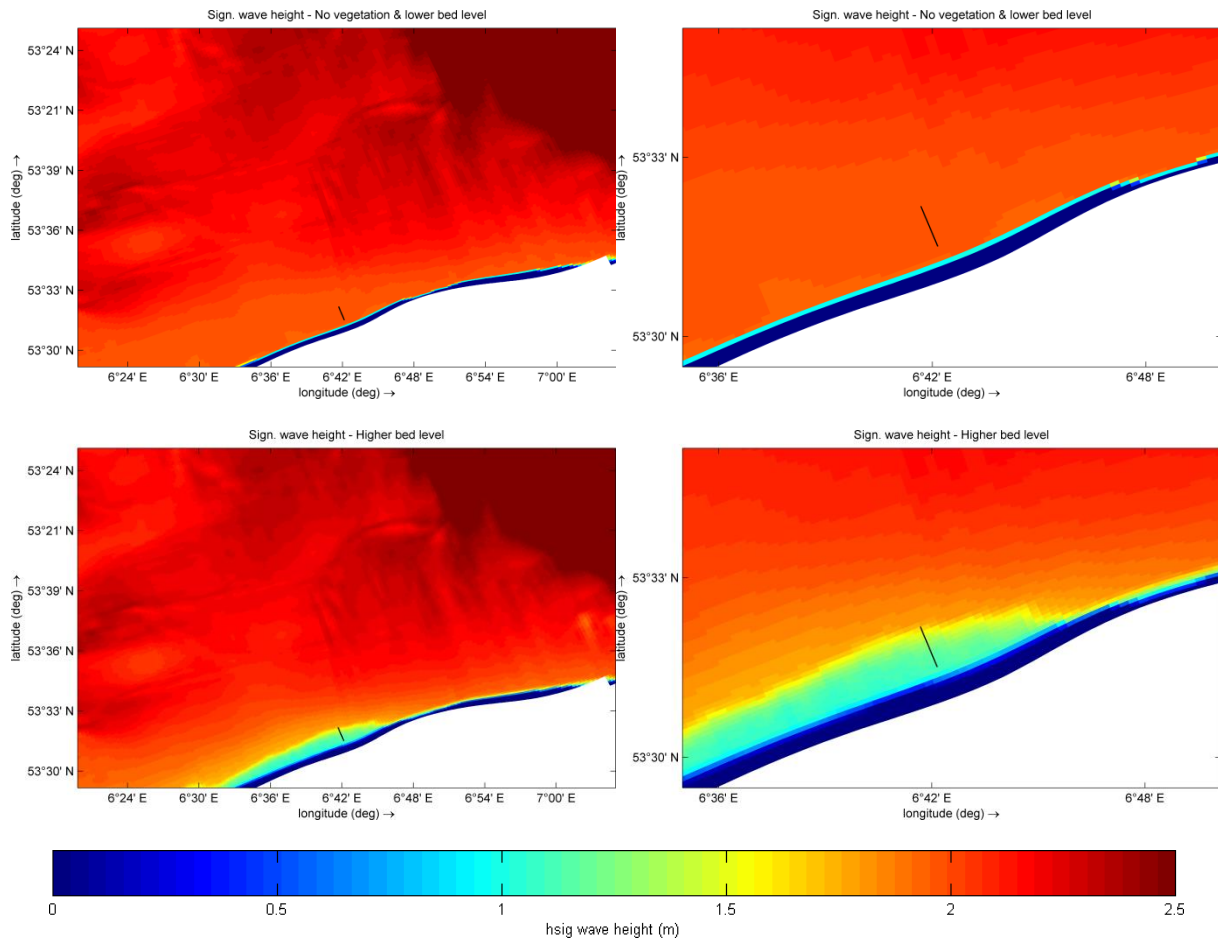


**Figure 61** An overview of the significant wave height for the different scenarios. From top to bottom: Current situation, larger salt marsh, no vegetation, no vegetation and lower bed level, higher bed level.

### Impact of salt marshes on the 2% wave run-up

Using the results from the current situation under design conditions, it is possible to calculate the 2% wave run-up  $R_{u2\%}$  under those conditions. This illustrates the impact of vegetated foreshores on dike safety (Figure 62). The maximum difference in  $R_{u2\%}$  found between the vegetated and non-vegetated areas is 2.03 m, or a reduction of 41%.

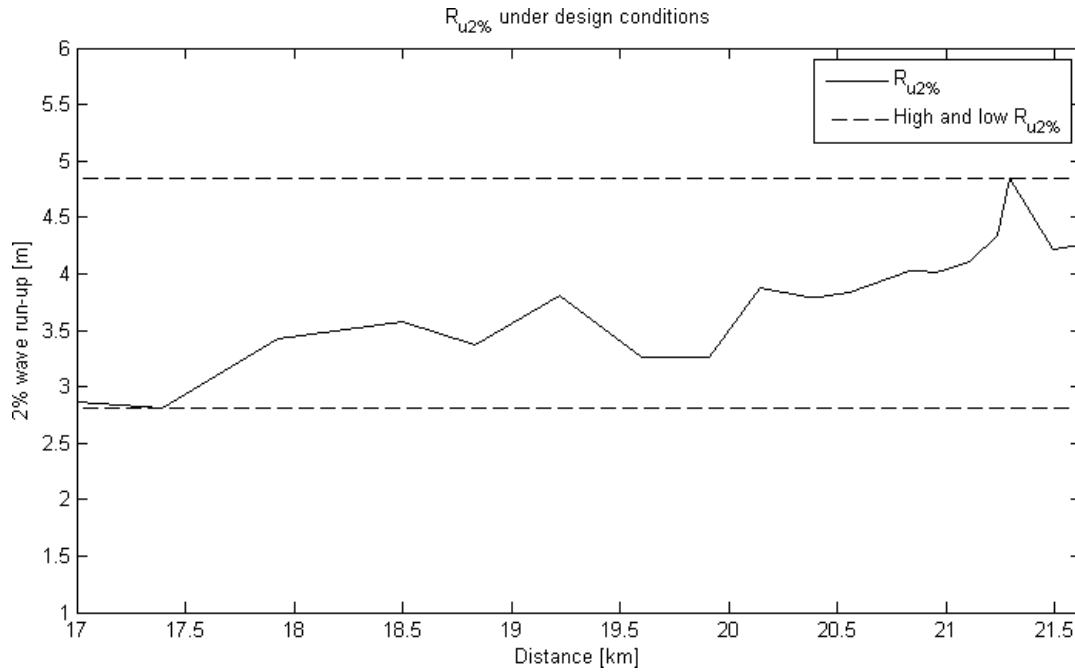


Figure 62  $R_{u2\%}$  under design conditions. The maximum difference in  $R_{u2\%}$  along the dike is 2.03 m

## 7. Discussion

The salt marshes have a large influence of the wave conditions in front of a dike during a storm event with a 1/4000 yearly probability. The results show that the wave heights are reduced significantly which increases the local safety. All dikes are designed to have a certain life expectancy and need to be strengthened or heightened after this period. By taking the impact of the salt marshes into account, this large scale maintenance can be postponed by possibly several tens of years, saving several million euros per kilometer. The salt marshes reduces the probability of most failure mechanisms such as stability of the slopes, wave overtopping and even piping (Venema et al., 2012). The marshes are also sea-level-rise-proof since higher water levels will result in more sedimentation.

In this research, the influence of the different properties of a salt marsh were investigated with respect to wave damping. It is found that the extent of the salt marshes is less important than the bed level and presence of vegetation. Maintenance should therefore be focused on maintaining and increasing the bed level of the salt marsh to further improve the safety. The difference in bed level between a vegetated area and a barren one, is approximately 1000 m<sup>3</sup> per m of shoreline. This is the amount of soil that is needed on average to create salt marshes for the rest of the shore.

The 1D model is entirely based on wave measurements performed with the pressure sensors located on the salt-marsh, perpendicular to the dike. The 1D model assumes that waves travel in a straight line along the grid. However, the waves registered by the pressure sensors arrived at an angle, which cannot be determined from the measurements since the sensors only record pressure. This means that the waves which were measured near the dike, travelled 15% further over the salt-marsh than the length of the model. When calibrating the dissipation terms, the  $C_D$  and  $K_N$  values are overestimated, possibly leading to unreliable results when the model is extrapolated to the design conditions.

In the 1D scenarios, a discrepancy is found between the scenario where the vegetation is simulated as additional bed roughness and where the vegetation is simulated as vertical cylinders with a certain drag factor. What is shown is that the  $H_{m0}$  is 8 cm higher at the toe of the dike when vegetation is seen as additional bed roughness. One (or both) of the two setups is over- or underestimating the real dissipation. In the 2D model, the vegetation is always schematized as bed roughness, since the version of SWAN which is required for the vertical cylinders approach is not yet available in Delft3D. This means that the  $H_{m0}$  values calculated in the 2D scenarios with the hydraulic boundary conditions are possibly

overestimated for locations with vegetation. The effect of the dissipation over the salt marshes is therefore possibly higher than what is calculated in the 2D scenarios.

Both models are calibrated using measurements of a single storm. Unfortunately, there are no other measurements of storms on the salt marshes, which means that no validation of the models was possible. The accuracy of the models is therefore unknown for other conditions than the measured storm of January 11<sup>th</sup> 2015. This also means that it is uncertain how accurate the models are when scaled up to design conditions where the water depth, wind speed and wave conditions are increased.

The flotsam levels are reproduced to a certain degree but several issues were encountered. Firstly, the measurements have an estimated accuracy of  $\pm 0.4$  m due to the local variability of the flotsam on the dike. Secondly, the calculation for the maximum wave run-up which is compared to the flotsam levels also knows several inaccuracies. The values for  $H_{m0}$  and  $T_{m-10}$  are used in the run-up calculation and determined using the 2D model. In the evaluation of the 2D model it became clear that especially  $T_{m-10}$  is underestimated for the shallow areas near the dike. Thirdly, it remains uncertain how the 2% wave run-up compares to the maximum wave run-up. The local variation in wave conditions which was seen in the flotsam measurements was not entirely reproduced by the 2D model. This means that the combination of flotsam level measurements, model results and the method to calculate the maximum wave run-up is too inaccurate to calibrate a wave model. However, the flotsam levels are still a useful indicator of how the wave conditions vary spatially during a storm as was seen in Chapter 3.3.

## 8. Conclusions and recommendations

At the start of this research three research questions were formulated. The first question is: *How do the salt marshes in the eastern Wadden Sea affect the wave conditions at the dike under design conditions?* The answer to this question is determined in 1D and 2D for both the measured storm of January 11<sup>th</sup> 2015 and the local design conditions. The influence of the vegetated foreshore is significant. Comparing the significant wave height at the toe of the dike at the salt marsh with locations without vegetation and a lower bed level, the difference in for  $H_{m0}$  near the dike is between 27% and 36% for the 1/4000 year storm. The salt marsh also lowers the wave period  $T_{m-1,0}$  which leads to a lower wave run-up. The 2% wave run-up is decreased by up to 41% due to the presence of the salt marsh.

The vegetation on the salt marshes is important for the amount of wave damping. Vegetation reduces the significant wave height by an additional 15% and 50% compared to a foreshore without vegetation. The bed level found in front of the dike also has a large influence on the waves for two reasons. Firstly because the reduced water depths cause the larger waves to break, limiting the height of the waves reaching the dike. Secondly, bed levels above the mean flood level are required for the type of vegetation found on the salt marshes.

The results suggest that the current extent of the vegetation at the test site in seaward direction is sufficient. The first reason for this is the fact that the significant wave height is dampened only slightly close to the dike, which means that the situation is close to an equilibrium between the wind which adds energy the waves, and the dissipative terms. The second reason is that extending the marsh further into sea by 1500 meters results in limited additional wave damping.

The second research question was: *Can flotsam measurements serve as field evidence for wave run-up reduction by vegetated foreshores?* To answer this, the flotsam measurements were compared with the foreshore bed level and the extent of the vegetation (or: the distance from dike to the edge or the marsh). These parameters represent the variation in the vegetated foreshores. The correlation between the foreshore bed level and the extent of the vegetation is high, which confirms that the two are related since the vegetation requires a certain bed level and vegetation improves sedimentation. The vegetation extent and bed level are highly correlated to the flotsam level, reducing the flotsam level when the other parameters increase. Due to the high correlation between the flotsam level and the vegetated foreshore characteristics and the knowledge that the flotsam levels are determined by the local maximum wave run-up, it is possible to say that the flotsam levels can certainly serve as an indicator for the run-up reduction by vegetated foreshores.

The final research question was: *Can flotsam measurements be approximated using a 2D wave model?* The 2D model which was created in this research was used to determine the water level and wave conditions near the dike for all flotsam measurements. Using this information, the local maximum wave run-up could be determined (Chapter 5). The pattern found in the flotsam measurements could be reproduced well. The values of individual measurements were replicated with the maximum wave run-up calculations, but only when taking both measurement ( $\pm 0.4$  m) and model uncertainties into account ( $\pm 20\%$ ). This means that the flotsam levels can be approximated using a 2D model and are useful as an indicator of local wave conditions but cannot be used to calibrate a 2D model due to the seeming inherent uncertainties related to the flotsam levels.

It is possible to make several recommendations based on this thesis for future research. Firstly it is very interesting to investigate the influence of the method to schematize vegetation. In the 1D model it became clear that when extrapolating from a calibrated situation to the design conditions, the ‘vegetation as additional bed friction method’ leads to less dissipation than the vertical cylinders method. However, the vertical cylinders method is not yet available in Delft3D-WAVE and could therefore not be tested. This can be overcome by replacing the version of SWAN manually and entering the SWAN commands via a separate script. The alternative is to wait for Delft3D to incorporate these features into the standard version which will likely be available at some point in the future.

Secondly, it would be interesting to compare the calibrated models for different storms. This must be done by placing pressure sensors on the salt-marsh to measure the wave conditions, since wave measurements on the salt marshes are normally not performed. It is important to measure two storms within a time period where the vegetation characteristics changes are limited. By validating the model against a second storm, the dissipation by vegetation can be estimated with more certainty, leading to a higher confidence when scaling the model to the design conditions.

Thirdly, the schematization of the vegetation is based on a single biomass measurement of the vegetation and estimation from literature and photos. Having more and more accurate measurements of the vegetation could possibly add a lot of detail to the schematization of the vegetation. The values that should be determined are the average stem diameter, vegetation height and the biomass.

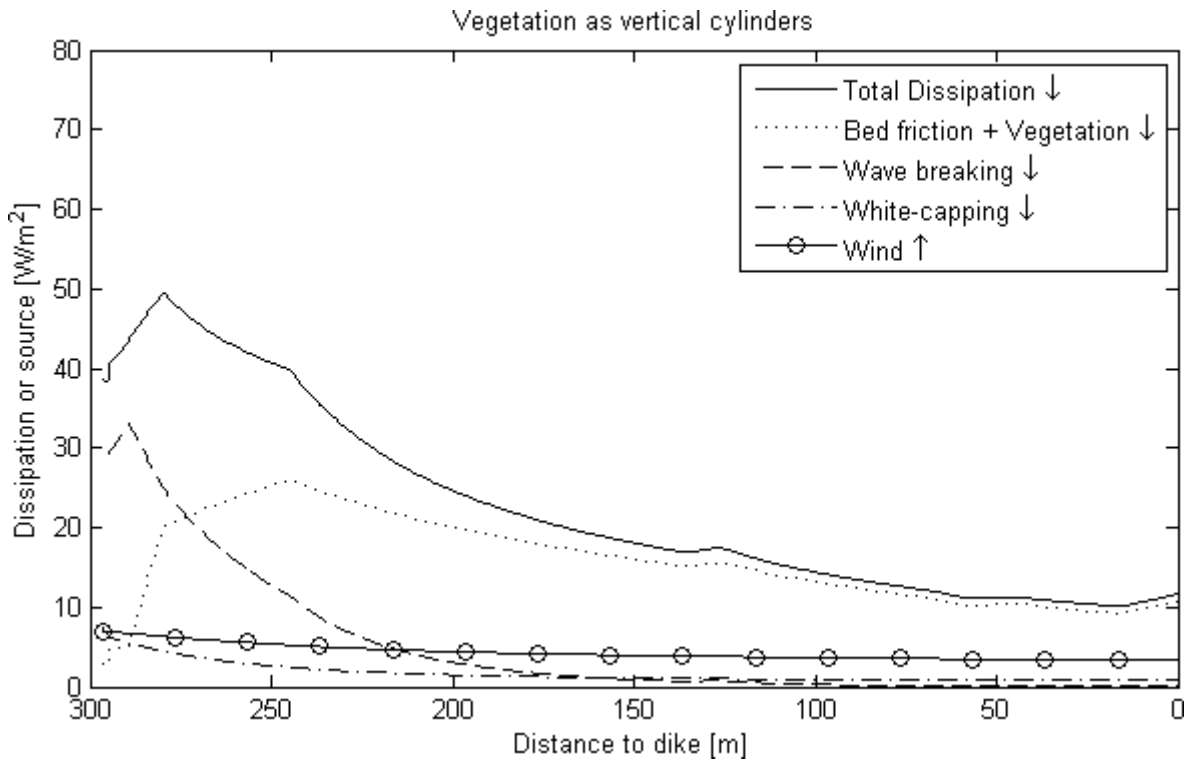
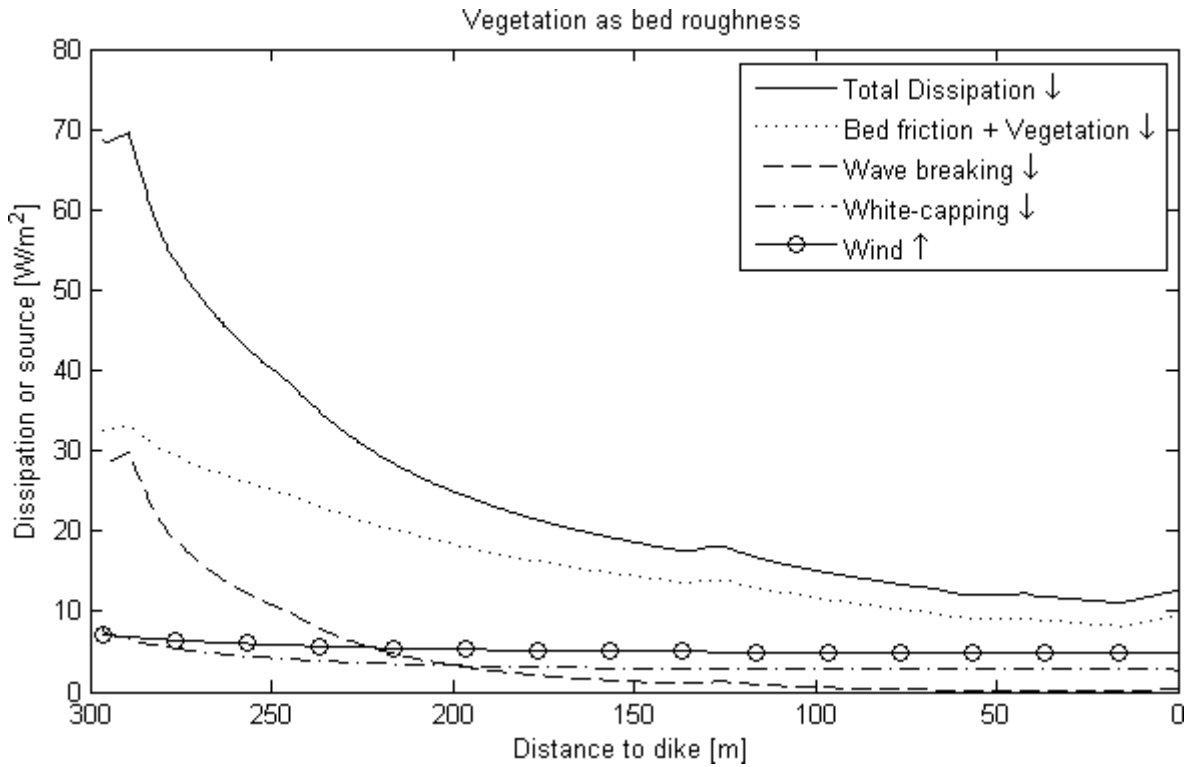
Finally, all wave calculations were performed in stationary mode. Comparing what the difference in  $H_{m0}$  is in the two approaches would be interesting.

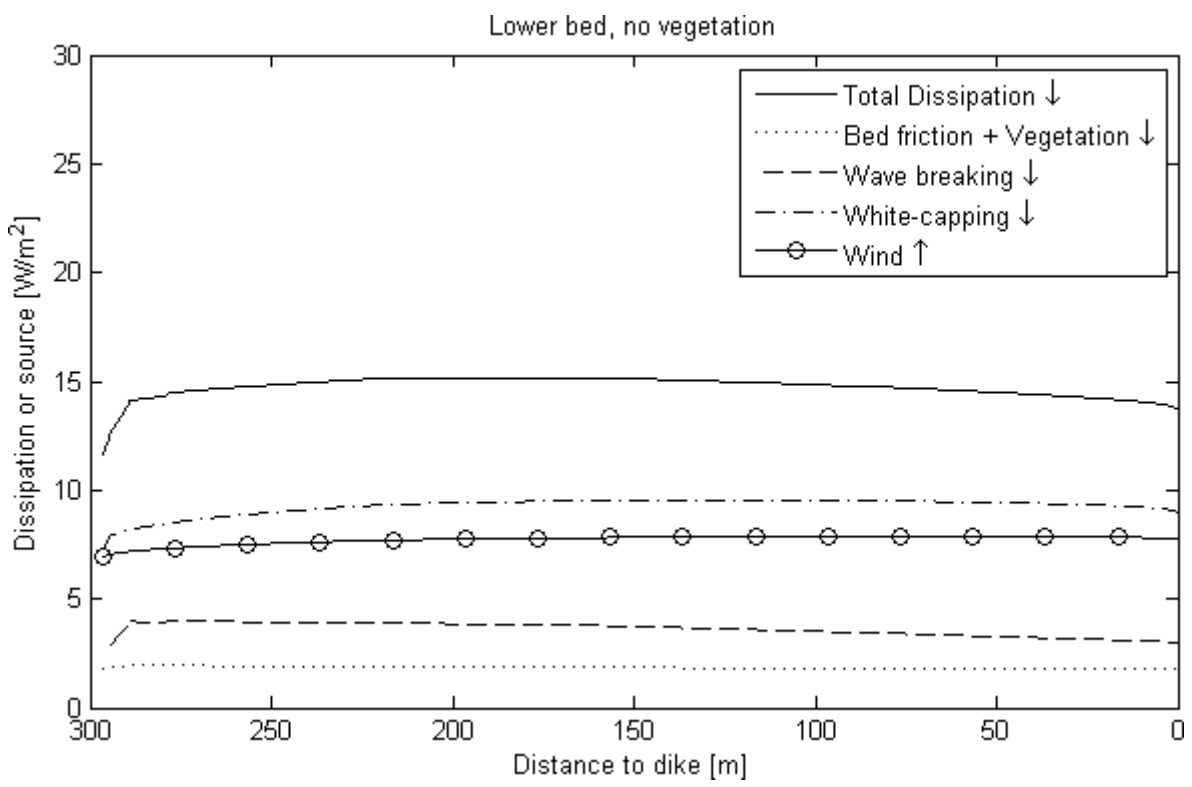
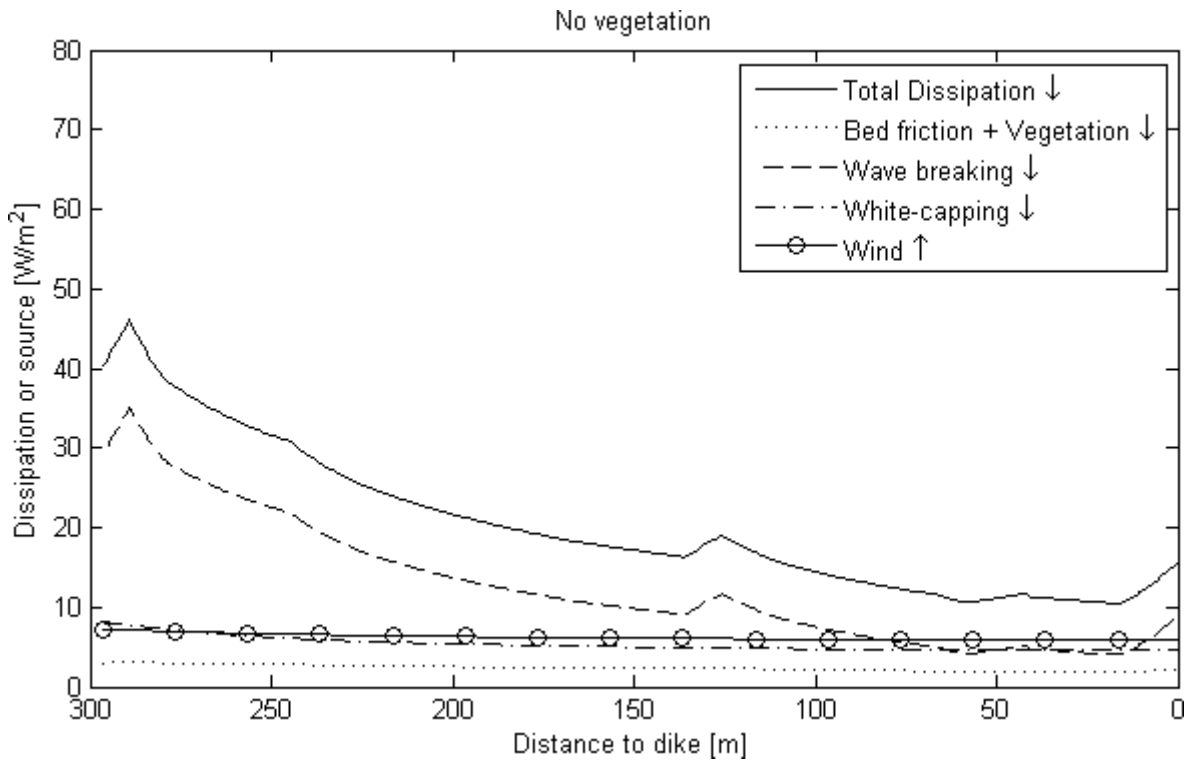
## References

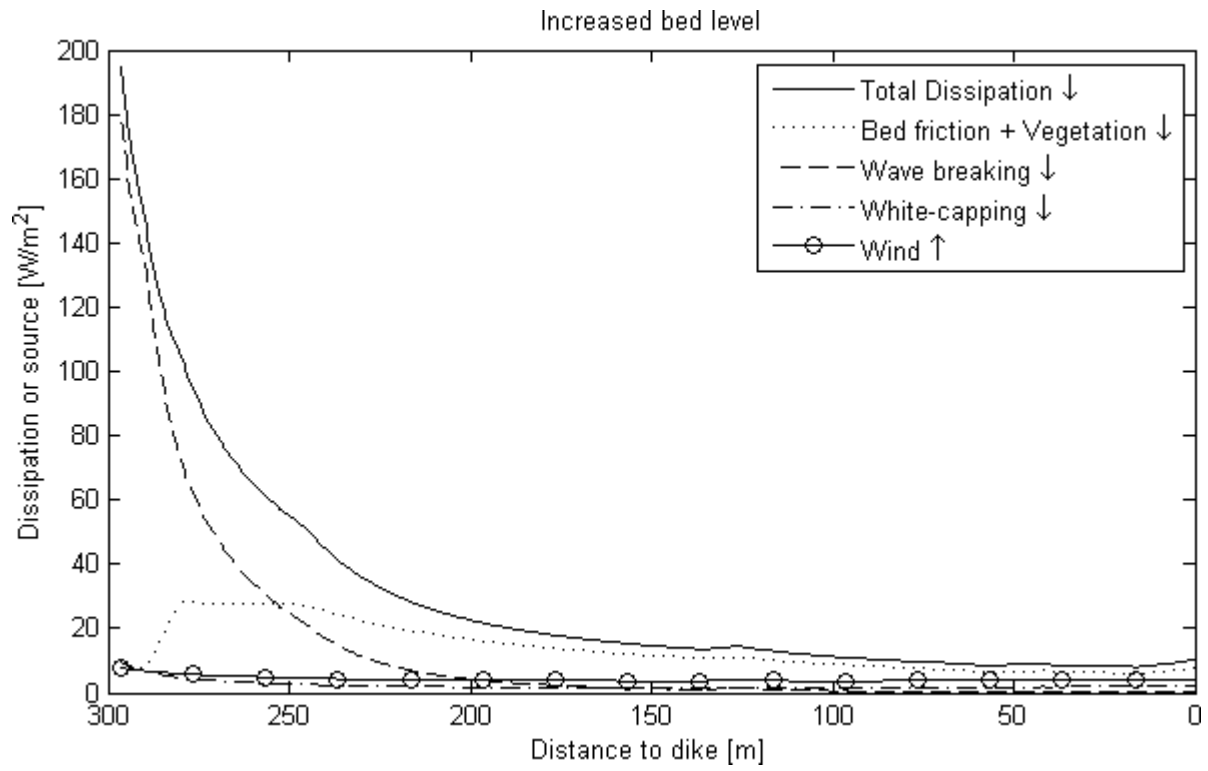
- Adema, J., Geleynse, N., & Telenta, B. (2014). *Een rekenexperiment voor de waddenzee, de storm van 5 & 6 december 2013*.
- Anderson, M. E., & Smith, J. M. (2014). Wave attenuation by flexible, idealized salt marsh vegetation. *Coastal Engineering*, 83, 82–92.
- Bradley, K., & Houser, C. (2009). Relative velocity of seagrass blades: Implications for wave attenuation in low-energy environments. *Journal of Geophysical Research: Earth Surface*, 114.
- Buckley, M., & Lowe, R. (2013). Evaluation of nearshore wave models in steep reef environments. *Coastal Dynamics*, 249–260.
- Butler, L. D., Cropper, J. B., Johnson, R. H., Norman, A. J., Peacock, G. L., Shaver, P. L., & Spaeth, K. E. (2006). *National range and pasture handbook*. USDA.
- Collins, J. I. (1972). Prediction of shallow-water spectra. *Journal of Geophysical Research*.
- Cronin, K., & Bing Wang, Z. (2012). *Analyse lidar data voor het Friesche Zeegat*. Deltares.
- De Reus, J. H. (1983). *Reactie op het rapport: Analyse van vloedmerkwaarnemingen op de dijk onder Hollum op Ameland*. Rijkswaterstaat.
- Dijkema, K. S., Duin, W. E. Van, Dijkman, E. M., & Leeuwen, P. W. Van. (2007). *Monitoring van kwelders in de Waddenzee*. Wageningen.
- Dissanayake, P., Kurunaratna, H., & Ranasinghe, R. (2015). Numerical modelling on sea level rise on large tidal inlet/basin systems. In *E-Proceedings of the 36th IAHR World Congress* (pp. 1–9). The Hague.
- Donker, J. (2015). *Hydrodynamic processes and the stability of intertidal mussel beds in the Dutch Wadden Sea*. University of Utrecht.
- Eldeberky, Y., & Battjes, J. A. (1996). Spectral modeling of wave breaking: Application to Boussinesq equations. *Journal of Geophysical Research*.
- EurOtop. (2007). *Wave overtopping of sea defences and related structures: Assessment manual*.
- Fischenich, C., & Dudley, S. (1999). Determining drag coefficients and area for vegetation. *Ecosystem Management and Restoration Research Program*, 2(2).
- Grüne, J. (2005). Evaluation of wave climate parameters from benchmarking flotsam levels. *International Conference on Coastlines, Structures and Breakwaters*, 1–10.
- Hasselmann, K., Barnett, T. P., Bouws, E., Carlson, H., Cartwright, D. E., Enke, K., ... Walden, H. (1973). Measurements of wind-wave growth and swell decay during the Joint North Sea Wave Project (JONSWAP). *Ergänzungsheft Zur Deutschen Hydrographischen Zeitschrift Reihe, A(8)*, p.95.

- Hasselmann, K., & Collins, J. I. (1968). Spectral dissipation of finite depth gravity waves due to turbulent bottom friction. *Journal of Maritime Research*, 26, 1–12.
- Holthuijsen, L. (2007). *Waves in oceanic and coastal waters*. *Oceanography*.
- Horstman, E. M., Dohmen-Janssen, C. M., Narra, P. M. F., van den Berg, N. J. F., Siemerink, M., & Hulscher, S. J. M. H. (2014). Wave attenuation in mangroves: A quantitative approach to field observations. *Coastal Engineering*, 94, 47–62.
- Hu, Z., Stive, M. J. F., & Zitman, T. J. (2012). *Drag coefficient of vegetation in flow modeling*. *Coastal Engineering Proceedings*. Delft University of Technology.
- Hwang, P. A. (2005). Temporal and spatial variation of the drag coefficient of a developing sea under steady wind-forcing. *Journal of Geophysical Research*, 110.
- IJnsen, F. (1983). *Analyse van vloedmerkwaarnemingen op de dijk onder Hollum op Ameland*. Rijkswaterstaat.
- Kaminsky, G. M., & Kraus, N. C. (1993). Evaluation of depth-limited wave breaking criteria. In *Proceedings of 2nd International Symposium on Ocean Wave Measurement and Analysis* (pp. 180–193).
- Lövstedt, C. B., & Larson, M. (2010). Wave damping in reed: Field measurements and mathematical modeling. *Journal of Hydraulic Engineering*, 136, 222–233.
- Madsen, O., Poon, Y., & Graber, H. (1988). Spectral wave attenuation by bottom friction. *Coastal Engineering*, 492–504.
- Mendez, F. J., & Losada, I. J. (2004). An empirical model to estimate the propagation of random breaking and nonbreaking waves over vegetation fields. *Coastal Engineering*, 51, 103–118.
- Padilla-Hernández, R., & Monbaliu, J. (2001). Energy balance of wind waves as a function of the bottom friction formulation. *Coastal Engineering*, 43, 131–148.
- Ridderinkhof, H. (1990). *Residual currents and mixing in the Wadden Sea*. University of Utrecht.
- Smale, A. (2010). *Hindcast of the flotsam levels of the 1 November 2006 storm in the Eastern Wadden Sea*. Witteveen+Bos.
- Smith, J. (2004). Shallow-water spectral shapes. In *29th International Conference Coastal Engineering* (pp. 206–217).
- Venema, J. E., Schelfhout, H. A., Moerman, E., & van Duren, L. A. (2012). *Kwelders en dijkveiligheid in het Waddengebied*.
- Walker, R. (2014). SI materials. Retrieved July 1, 2015, from [www.simetric.co.uk/si\\_materials.htm](http://www.simetric.co.uk/si_materials.htm)

## Appendix A: Source terms of the 1D scenarios







## Appendix B: Source terms of the 2D scenarios

